Coordinated Control of MVDC Shipboard Microgrids with Pulsed Power Loads

Xu, Luona

DOI (link to publication from Publisher):
10.54337/aau499832422

Publication date:
2022

Document Version
Publisher's PDF, also known as Version of record

COORDINATED CONTROL OF MVDC SHIPBOARD MICROGRIDS WITH PULSED POWER LOADS

BY
LUONA XU

DISSERTATION SUBMITTED 2022

AALBORG UNIVERSITY
DENMARK

COORDINATED CONTROL OF MVDC SHIPBOARD MICROGRIDS WITH PULSED POWER LOADS

by

Luona Xu

AALBORG UNIVERSITY
DENMARK

Dissertation submitted

.

Dissertation submitted: August, 2022

PhD supervisor: Prof. Josep M. Guerrero
Aalborg University

Assistant PhD supervisor: Prof. Juan C. Vasquez
Aalborg University

Asst. Prof. Baoze Wei
Aalborg University

PhD committee: Associate Professor Jayakrishnan Radhakrishna Pillai (chair)
Aalborg University, Denmark

Professor Olav Bjarto Fosso
Norwegian University of Science and Technology, Norway

Associate Professor Ir.Ts. Dr. Muzamir Iza,
Universiti Malaysia Perlis, Malaysia

PhD Series: Faculty of Engineering and Science, Aalborg University

Department: AAU Energy

ISSN (online): 2446-1636
ISBN (online): 978-87-7573-840-3

Published by:
Aalborg University Press
Kroghstræde 3
DK – 9220 Aalborg Ø
Phone: +45 99407140
aauf@forlag.aau.dk
forlag.aau.dk

Printed in Denmark by Stibo Complete, 2022

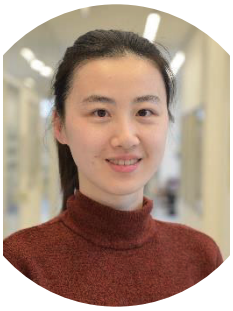

CV

Luona Xu received the B.S. degree in Electrical Engineering and Automation from China Agricultural University in 2014, and M.S. degree in Electrical Engineering from University of Chinese Academy of Sciences in 2017. From 2017 to 2019, she was an electrical engineer at East China Electric Power Design Institute Co., Ltd., China. She is currently working toward her Ph.D. degree at AAU Energy, Aalborg University, Denmark, as part of the Villum Center for Research on Microgrids (CROM).

Her research interests focus on the application of power electronics in power grids and electrification transportation, including microgrids, power converters for renewable generation systems, electromobilities and charging stations.

ABSTRACT

Electric ships are obtaining much attention in reducing greenhouse gas emissions and achieving clean water transportation. In most cases, shipboard power systems are regarded as shipboard microgrids (SMGs) due to their islanding operation. The concept of DC SMG is popular in academia and industry since it has many merits compared with the AC counterpart, such as reduced fuel consumption, flexibility in generation integration, and compact system design. Some research on DC SMGs has been done in recent years, while there are still several open questions for high-power, efficient, flexible, and reliable ship operation. Thus, this thesis introduces a comprehensive overview of medium voltage DC (MVDC) SMGs, presenting the system configuration and control issues and highlighting the technical particularities compared to microgrids in other applications. In light of the investigation, two topics are focused on in this thesis: the proper control methods on the generation side and the power supply subsystem for pulsed power loads (PPLs), which is a particular load type in ships.

The overview of MVDC SMGs presents the hardware configuration of electric ships based on the DC network and the associated system control issues. The general system architecture and power components are reviewed and analyzed, and then the suitable applications of each type are discussed. Regarding control issues, the overall control schemes for the generators and the energy storage systems (ESSs) in ships are presented. Besides, due to the stability issues as well as the protection systems in MVDC SMGs are still rarely studied, particular concerns on these two topics for maritime application are discussed.

The coordinated control of synchronous generators and ESSs in electric ships is developed. The DC network enables variable-speed operation of generators, therefore allowing the optimization of the generator speed to achieve different objectives, which is managed in the energy management system (EMS). Additionally, the integration of ESS makes it flexible in power sharing. However, these studies do not consider the cases of the ships operating in different operation modes under various load conditions. To fill this research gap, the coordinated control should be well designed to fit each mode. This thesis presents a coordination method for synchronous generators and batteries. In the proposed approach, hybrid-electric and all-electric operation modes are considered to meet different operation scenarios, and flexible mode switching can be achieved. Besides, the state of charge balance between battery packs is considered to avoid overcharge and over-discharge of batteries.

The power supply for PPLs is a challenge in DC SMG control, as the PPL absorbs enormous transient power and requires a fast dynamic response. Shipboard PPLs could be high-power pulse radars and electromagnetic railguns, which are vital for naval vessels. The confidentiality of military applications makes it difficult to obtain the technical details of existing PPLs. This thesis studies the impacts of the PPL

parameters on the bus voltage and based on these, the control method of a pulsed power supply (PPS) system is developed. An improved approach based on sliding mode control (SMC) is adopted. Simulation results verify the effectiveness in terms of dynamic response and robustness.

In summary, the contributions of this Ph.D. project aims to explore the overall configuration and control of DC SMGs, and then present coordinated control strategies for generators and ESSs as well as the control of the power supply subsystem in the presence of high power PPLs. These works are anticipated to pave the way for the broader implementation of MVDC SMGs in industry and naval applications.

DANSK RESUMÉ

Elektriske skibe får stor opmærksomhed i baggrunden for at reducere drivhusgasemissioner og opnå emissionsfri vandtransport. Skibskraftsystemet fungerer i ø-tilstand og kan således ses som en shipboard mikrogrid (SMG). Konceptet DC SMG har mange fordele sammenlignet med AC-modstykket, såsom reduceret brændstofforbrug, fleksibilitet i generationsintegration og kompakt systemdesign, hvilket gør det populært i både den akademiske verden og industrien. En del af undersøgelser om DC SMG'er er udført i de seneste par år, mens der stadig er flere spørgsmål om effektiv, fleksibel og pålidelig skibsdrift. Derfor introducerer denne afhandling et omfattende overblik over mellemspænding DC (MVDC) SMG'er, der præsenterer systemkonfiguration og kontrolproblemer, og fremhæver de tekniske egenskaber i sammenligning med mikrogrid i andre applikationer. Fokuserer derefter på to spørgsmål: de korrekte styringsmetoder på generationssiden og strømforsyningsundersystemet for pulserende strømbelastninger (PPL'er), som er en særlig belastningstype i skibe.

Oversigten over MVDC SMG'er præsenterer hardwarekonfigurationen af elektriske skibe baseret på DC-netværk og de tilhørende systemkontrolproblemer. Den generelle systemarkitektur og strømkomponenter gennemgås og analyseres, og derefter diskuteres de egnede anvendelser af hver type. De overordnede kontrolordninger for generatorer og energilagringssystem (ESS) i skibe præsenteres. Da stabilitetsspørgsmålene og beskyttelsessystemet i DC SMG'er stadig sjældent studeres, diskuteres særlige bekymringer vedrørende disse to emner for maritim anvendelse.

Den koordinerede kontrol i elektriske skibe for synkrongeneratorer og ESS'er, præsenteres. DC-netværket muliggør drift med variabel hastighed af generatorer, hvilket gør det muligt at optimere generatorhastigheden for at opnå forskellige mål, som styres af energistyringssystemet (EMS). Derudover gør integrationen af ESS den fleksibel i deling af effekt. Disse undersøgelser tager dog ikke højde for tilfældene af skibe, der opererer i forskellige driftstilstande under forskellige lastforhold. For at klare dette problem bør den koordinerede kontrol være godt designet til at passe til hver tilstand. Denne afhandling præsenterer en koordinering for synkrongeneratorer og batterier. I den præsenterede metode anses hybrid-elektriske og alt-elektriske driftstilstande for at opfylde forskellige driftsbetingelser, og jævnt tilstandsskift kan opnås. Desuden tages der hensyn til ladetilstandsbalancen mellem batteripakker for at undgå overopladning og overafladning af batterier.

Strømforsyningen til PPL'er er en udfordring i DC SMG-styring, da PPL'en absorberer stor transient effekt og kræver hurtig dynamisk respons. PPL'er om skibebord kunne være højeffektpulsradarer og elektromagnetiske jernbanekanoner, som er afgørende for flådefartøjer. Fortroligheden af militær anvendelse gør det vanskeligt at få fat i de tekniske detaljer for eksisterende PPL'er. Denne afhandling studerer PPL-

parametrenes indvirkning på busspændingen, og baseret på disse udvikles styringsmetoden for et pulseret strømforsyningssystem (PPS). I den præsenterede metode er en forbedret metode baseret på sliding mode control (SMC) vedtaget. Simuleringsresultater bekræfter effektiviteten med hensyn til dynamisk respons og robusthed.

Bidragene af denne ph.d. projektet er at sigte mod at udforske styringen af DC SMG'er og derefter præsentere koordinerede styringsstrategier for generatorer og ESS'er samt styringen af strømforsyningsundersystemet i nærværelse af højeffekt PPL'er. Det forventes, at disse arbejder viser en større mulighed for implementering af DC SMG'er i industri- og flådeapplikationer.

PREFACE

This Ph.D. project is a summary of the outcomes from the project '*Coordinated Control of MVDC Shipboard Microgrids with Pulsed Power Loads*', carried out at the CROM group at AAU Energy, Aalborg University, Denmark.

My sincere gratitude goes to my supervisor, Josep M. Guerrero, for giving me the opportunity to be part of his group. I would also thank my co-supervisors Juan C. Vasquez and Baoze Wei for their guidance, support, and patience during my Ph.D. study. It has been a great experience to work under their supervision.

Special thanks to Professor Jose Matas Alcala for hosting my visiting research at the Technical University of Catalonia, Spain, and giving me professional guidance and discussions. Also, thanks to Jorge El Mariachet Carreño at UPC for his kindness and for giving me living support in Barcelona.

I would like to thank my colleagues and friends at AAU for their kind support and exciting discussions. Thank all the staff at AAU Energy for their assistance during my Ph.D. study.

Last but not least, I would like to thank my parents and family for their endless love, care, and support throughout my study abroad.

Luona Xu
August 2022

.

CONTENTS

Report

CHAPTER 1. INTRODUCTION

1.1. BACKGROUND

Maritime transport plays a vital part in addressing climate change and creating a sustainable future. In 2021, the European Commission adopted a series of legislative proposals intending to reduce greenhouse gas (GHG) emissions by 55% by 2030, and further achieve climate neutrality in the European Union (EU) by 2050 [1]. It is also in line with the Paris Agreement aiming at slowing down the global temperature increase [2]. As 80% of worldwide trade is taken by marine transportation, the shipping industry is a sizable contributor to global GHG emissions [3]. With a significant market volume of nearly 100,000 commercial vessels globally, shipping takes up 3% of global carbon emissions [4]. In Europe, ships produced 13.5% of all GHG emissions from transport and emitted approximately 1.63 million tons of sulfur dioxide in 2019 [5], while the number of fleets is still increasing.

Ambitious goals are set to decarbonize the maritime industry. The International Maritime Organization (IMO) stated that by 2050, GHG emissions from international shipping should be cut 50% of that in 2008 [6]. As the executive director of the European environment agency (EEA) said, to have the shift toward a sustainable maritime transport sector, decarbonizing the maritime industry requires a systemic industry-wide transformation [7]. As a vanguard in shipping, Norway decreed in 2019 to make its protected fjords world's first zero-emission zones by 2026 [8]. A statistic on the European market size of electric cargo ships shows that over threefold growth is projected between 2018 and 2030, as shown in Figure 1-1 [9]. From a worldwide perspective, the global electric ship market grows from USD 5 billion in 2019 to over USD 10 billion by 2027 in estimation, and it is predicted to increase by about 1.3% annually till 2050 [10].

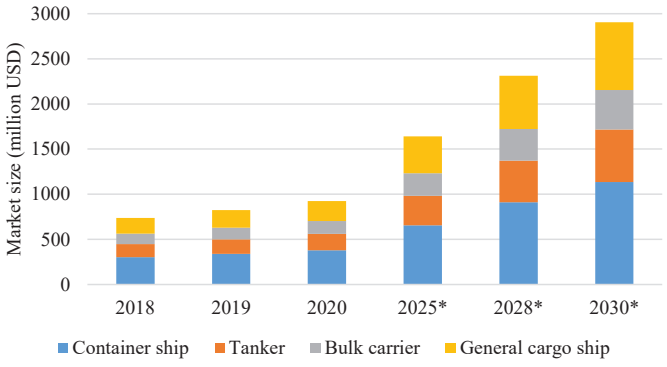

Figure 1-1 European market size for electric cargo size.

Shipbuilders and operators worldwide are moving from diesel-driven engines to hybrid and electric propulsion to achieve efficient, environmentally compatible, and flexible operation. In a mechanical propulsion system, the prime mover, typically an internal combustion engine, drives the propulsor directly or through a gearbox. While in an electric propulsion system, the motors are driven by controllable power converters, and the alternators feed a common bus [11]. The retrofit transition from fossil fuel-driven to all-electric usually needs to be taken in several phases. The Swedish Ro-Ro/passenger vehicle was converted to electric propulsion and introduced a 1MWh battery for bow thrusters and maneuvering in 2018, being one of the world's largest battery capacities in ships, and was projected to have about 50MWh more to achieve fully electric operation [12]. A few prominent companies, such as Wärtsilä (Finland), ABB (Switzerland), Kongsberg Maritime (Norway), and Danfoss Editron (Denmark) among others, are developing electric ships with advanced features of using clean energy sources and autonomous operation [13].

Developing all-electric ships is constrained by the onboard battery capacity and the charging infrastructures on the routes. Ferries that travel short distances and have proper turnaround time when they dock, and tugs that operate in a regular pattern with an extended time at dock, are ideally suited to fully electric [14]. In 2022, the world's first fully electric autonomous cargo ship 'Yara Birkeland' has set sail successfully supported by 6.8MWh onboard battery [15].

The development of electric ships has gone through the exploration of both AC and DC distributions. The first attempt to use electricity on ship was for lighting in the steamship 'SS Columbia' in 1880, and the supply system was powered by battery cells based on a DC network [16]. In the early 20th century, turbo-electric generation and distribution system in AC distribution became popular since it improved fuel economy and speed regulation flexibility more effectively than the DC networks [17]. A typical AC shipboard distribution is shown in Figure 1-2 (a). The generators feed the AC bus directly or through 50/60Hz transformers. Till the late 1990s, the development of solid-state power electronics made high power conversion possible. DC shipboard distribution re-attracts attention as it allows the integration of variable-speed generation with improved fuel efficiency, simplifies the connection of generator without phase angle synchronization issues, and makes the system more compact by removing the bulky transformers [18]. Figure 1-2 (b) shows a typical DC shipboard distribution. Both generators and propulsion motors, among other power components, connect to the DC bus through power converters, which bring flexibility in power regulation. With increasing load power demand and various operation scenarios in ships, MVDC shipboard power systems (SPSs) are more and more studied in academia and industry.

Besides the electric propulsion and shipboard electric system, critical enabling technologies in the electrification of the maritime industry include energy storage,

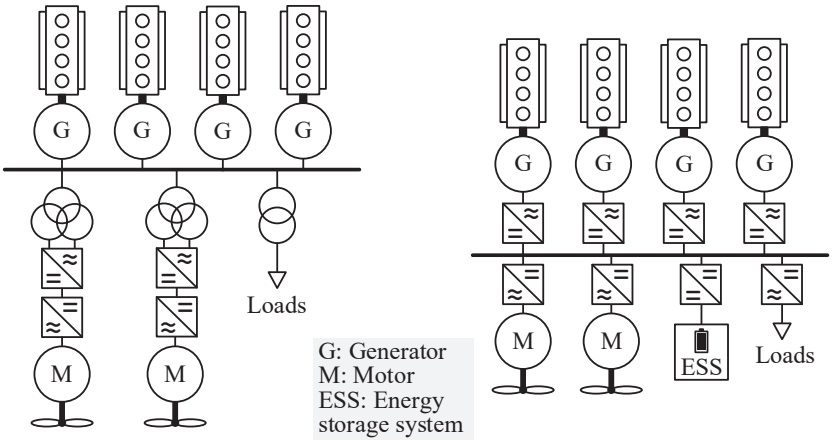

(a) Traditional AC SMG (b) Typical DC SMG

Figure 1-2 Typical system layout of AC and DC SMGs.

onshore charging, fuel cells (FCs) and so on, which are popular research topics recently.

1.1.1. MVDC SMG CONCEPT

In modern electric ships, as the electric propulsion system together with other shipboard loads are fed by the common buses, the SPSs are also called the integrated power systems (IPSs) [19]. Generally, the IPS operates in islanding mode during the voyage, without the support from onshore power grids, while only the onboard power sources feed the bus. When the ship berths at dock, the SPS is connected to the onshore grid and gets charged, which is named cold ironing [20], [21]. Similar to terrestrial microgrids in system composition and operation, SPSs are also defined as shipboard microgrids (SMGs). A typical SMG consists of generation modules, energy storage system (ESS), electric propulsion system, payloads, and interface to onshore grids.

Compared with terrestrial DC microgrids (MGs), DC SMGs have the following differences, which motivate special considerations in designing and controlling the systems.

- From the aspect of the operation environment, the SMGs suffer a harsher operation environment with humidity, vibration, and compact component arrangements. Therefore, the reliability and robustness requirements in DC SMGs are much higher than those in terrestrial MGs [22]. Also, due to the limited space in ships, the DC SMGs require higher power density and smaller power components than the terrestrial MGs [23].
- From the aspect of load side, the load profile of SMGs is more unpredictable since the operation scenarios of ships are more complicated, such as suffering

Table 1-1. Recommended MVDC voltage classes (kV) [J1].

	MVDC Class	Nominal MVDC Class Rated Voltage	Maximum MVDC Class Rated Voltage
Established	1.5	1.5 or ±0.75	2 or ±1
	3	3 or ±1.5	5 or ±2.5
Future Design	6	6 or ±3	10 or ±5
	12	12 or ±6	16 or ±8
	18	18 or ±9	22 or ±11
	24	24 or ±12	28 or ±14
	30	30 or ±15	34 or ±17

harsh weather and wave conditions, and having military tasks for naval vessels. While the load profile in terrestrial MGs is more regular and predictable.

- From the aspect of power source side, to ensure power supply reliability, generators and batteries are still the primary energy sources for ships [24]. The application of FCs in ships is in research [25]. While terrestrial MGs may have a high penetration of renewable energies [26].
- From the aspect of ESS, hybrid ESS (HESS) that can provide both high power density and energy density are preferable for SMGs to meet the shipboard demand with fast dynamics and limited generation power [27]. While for terrestrial MGs, besides general energy storage devices, more forms of ESS can be adopted, such as Power-to-X (PtX) units [28], electro-thermal energy storage [29], and compressed air energy storage [30].

Medium voltage configuration is becoming popular due to increasing demands on power capacity up to megawatt rating and higher power density in various vessel types [18]. The voltage level depends on several factors, such as the voltage of generators and propulsion motors, onboard load demands, standard cable ratings, arc fault energy, and cost. In general, low voltage DC (LVDC) in shipping applications refers to lower than 1kV, while MVDC SMGs range from 1-35kV as suggested in IEEE Std 1709-2010 [31]. Recommended voltage classes for MVDC SMGs are presented in Table 1-1.

1.1.2. COORDINATED CONTROL IN MVDC SMGS

Hybrid-electric ships, which use engine-driven generators combined with ESSs, have been widely studied and designed over the last decades to achieve decarbonization and reduced-cost operation. Since high speed of vessels leads to significant fuel consumption and CO_2 emissions, optimized low speed is usually introduced in practice, resulting in the vessels spending a remarkable amount of time at low power [32]. Therefore, it is not cost-efficient to equip large diesel engines that are idling most of the time just to satisfy the maximum load demand, which only lasts

for a relatively short running hour. Instead, hybrid-electric configurations with the combination of smaller engines through a diesel-electric system and battery banks are increasingly adopted in the current shipping sector. This configuration is capable of providing power for long-distance sailing and short-term working with good demand matching and smooth operation by managing the load fluctuations placed on the engine. For specific vessel types, such as dynamically positioned vessels with dynamic positioning (DP) systems, hybrid power is particularly suitable for providing high power with dynamic flexibility.

Proper coordination between diesel generators and batteries is vital to address the challenges in providing stable and economical operation. For a SMG, without the system frequency constraint, one of the most critical control goals is to ensure the voltage stability. In addition to voltage regulation, various coordinated control objectives can be achieved, such as mitigating the transient voltage fluctuations [33], reducing the capacity of batteries and converters, therefore, minimizing the cost [34], and regulating the system frequency in AC/DC hybrid networks [35].

Generally, two coordinated control schemes manage the diesel generators and batteries to achieve voltage regulation and power management. In the first coordination scheme, as depicted in Figure 1-3, the wound field synchronous generators (WFSGs) are the primary power sources responsible for the DC bus voltage regulation by the excitation control. At the same time, the batteries compensate for the power unbalance between synchronous generators (SGs) and loads. The SGs connect to the DC bus via diode rectifiers with high reliability and low cost, and the excitation control regulates the output voltage. The governor adjusts the mechanical power by changing the rotating speed ω of the prime mover by regulating the fuel amount via the governor. The automatic voltage regulator (AVR) regulates the output voltage of the SG by controlling the exciter current to the excitation system [36]. The SG voltage v_{abc} has the amplitude of V_m calculated by (1.1):

$$V_m = \omega_e L_m i_f \tag{1.1}$$

in which ω_e is the electrical angular velocity, L_m is the magnetizing inductance of the SG, and i_f is the exciter current. Taking the commutation effect of diode-rectified SG into consideration, the DC output voltage of the diode rectifier v_{dc} is [37]:

$$v_{dc} = \frac{3\sqrt{3}}{\pi} V_m - \frac{3}{\pi} \omega_e L_s i_o \tag{1.2}$$

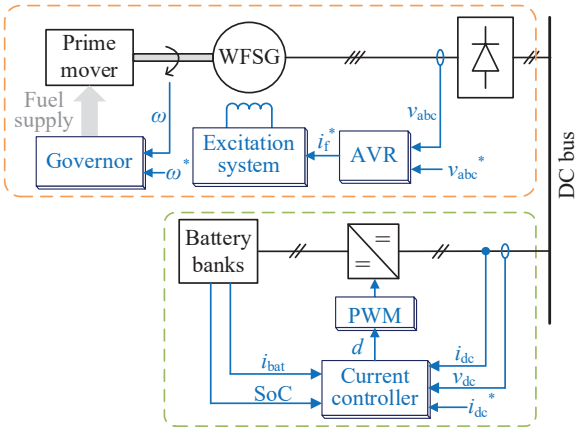

Figure 1-3 Coordination scheme with SG under excitation control.

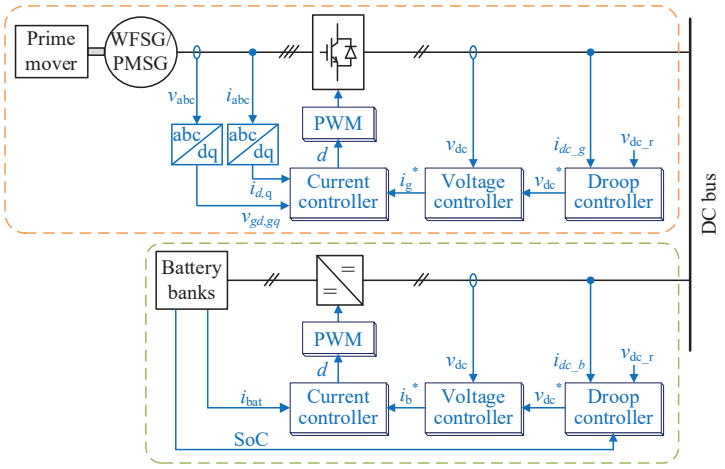

Figure 1-4 Coordination scheme under droop control.

where L_s is the SG synchronous inductance, i_o is the output DC current in the diode rectifier.

The control scheme based on SG excitation control benefits simple implementation and reliable operation. However, the large inertia in SGs results in a slow dynamic response in voltage regulation via the excitation system, and it brings difficulty in satisfying the fluctuating load profile of ships. Furthermore, from the aspect of fuel consumption, the slow dynamics make it hard to regulate the rotor speed accurately and instantaneously to achieve efficient operation [38].

The other coordination scheme is based on the decentralized droop control, shown in Figure 1-4, in which the bus voltage is regulated via the actively controlled converters, and the power sharing is achieved by adjusting the droop coefficient of each converter. Note that in the case of WFSG, instead of terminal voltage regulation, the objective of excitation control and speed control usually maximizes energy efficiency. In contrast, the excitation controller can be eliminated for permanent magnet SG (PMSG) [39]. Constraints of generator rated power, battery capacity, battery state-of-charge (SoC), ship operation mode and scheduling must be considered when designing the coordinated control strategies [40], [41]. A comparison of close-loop time constant of SG speed control, excitation control and the controller of the active rectifier shows the former has a decuple time constant of the latter one, so it can be seen as these three regulators are decoupled, and it can be stable if implementing three controllers [42].

1.1.3. PULSED POWER SUPPLY IN SMGS

Pulsed power loads (PPLs), such as radars, electromagnetic rail guns, aircraft launchers, etc., are special loads in vessels, particularly in naval ships [43]. Different from general service loads with relatively smooth power, PPLs have the load profile with very high transient power intermittently. The pulsed power usually ranges from tens of kilowatts to several megawatts, which even exceeds the onboard generation capacity in some cases, while the pulse duty cycles are typically lower than 10% [44], [45]. Thus, even though the peak power is very high, the average power of a PPL is relatively low, making the power supply for PPLs with economics a challenge. What is worse, the instantaneous high pulsed power presents severe issues in power quality and system reliability, such as voltage sag, voltage fluctuation, malfunction of system protection, and even system blackout [46].

An adequately designed pulsed power supply (PPS) subsystem is required to fulfill the PPL energy demand and reduce its adverse impacts on the system. A straightforward way is to add a dedicated ESS to provide transient power and suppress the voltage fluctuation [47]. To track the pulsed power, of which each pulse typically only lasts from several microseconds to seconds, the ESS has to be capable of discharging quickly. Ultra-capacitor (UC) and flywheel ESS (FESS) are good options as energy buffers due to their fast dynamics and high power density [43]. In terms of control strategy, existing PPSs are based on linear control methods such as proportional-integral (PI) control. However, the considerable power variation of PPL may result in the system operating point changing when the pulsed power is triggered and terminated. Therefore, nonlinear control methods are preferred in the PPS application. This Ph.D. project presents an improved PPS based on sliding mode control (SMC).

1.2. PROJECT MOTIVATION AND RESEARCH GOALS

As presented in the above section, hybrid-electric ships based on MVDC SMG configuration present merits in terms of power efficiency and operation flexibility, especially enabling the integration of PPLs. To fully exploit the benefits of MVDC SMG in a hybrid-electric ship, two research questions for this Ph.D. project are formulated:

- How to design the coordination strategy for generators and batteries to achieve efficient and flexible operation?
- How to control the PPS to provide a stable power supply with fast dynamics?

To answer above questions, some limitations in existing research have to be noted [35], [39], [48], [49]:

- Missing a comprehensive review on MVDC SMGs from the aspects of both system hardware schemes and control issues.
- Missing coordinated control methods for SMG based on DC configuration considering different operation scenarios.
- Missing the coordination of various battery packs according to their status to achieve reliable and fast SoC balance.
- Missing the analysis on impacts of PPL characteristics on the system performance.
- Missing the PPS with fast dynamics and robustness.

With these research gaps, this Ph.D. project aims at proposing solutions to remove the aforementioned limitations. Improved methods in terms of the coordinated control of generators and batteries and the control strategy for PPS are developed. The main goals of this dissertation are summed up as:

- **Investigate the MVDC SMGs from the aspects of both system configuration and control issues.**
  A comprehensive overview of the techniques on system configuration, control issues, and potential research challenges in MVDC SMGs are needed as this application is still in the infancy stage. Overview of the hardware aspect, including the system configuration and composition and the specific concerns in the MVDC SMG application in terms of the control issues, stability analysis, and system protection are summarized.
- **Develop the coordinated control strategy of SGs and battery packs.**
  The operation scenarios of ships and the operation characteristics of SGs and battery packs have to be considered in designing the coordinated control strategy to achieve stable and efficient system operation.
- **Develop the battery pack SoC balancing methods.**

The SoC balance among parallel connected battery packs in the DC SMG is necessary to avoid over-charging / over-discharging and hence to extend battery lifetime.

- **Analyse the impacts of PPL characteristics on the DC SMG performance.**
  It is known that the high power PPL may cause voltage stability issues, while how the PPL characteristics impact the DC SMG still need to be analysed, which is the basis for designing the control strategy of the PPS.
- **Develop improved control strategies for PPS with fast dynamic response and strong robustness.**
  According to the study of PPL impacts on system performance, which deduces the requirement on the PPS, an improved control method is proposed. Besides, the sizing of the PPS circuit components under the presented control strategy is analysed.

1.3. PROJECT LIMITATIONS

The SPSs vary from ship type, and the control systems are complicated. Some simplifications are made to simplify the system and focus on the problems this Ph.D. project aims at. Firstly, this thesis adopts the constant power control in the generator control to achieve specific objectives, though an energy management system (EMS) can also be implemented to optimize the generator operation with other optimization targets. Secondary, battery-cell level battery management is not considered in the SoC balancing control of battery packs. In practice, the battery pack consists of battery cells connected in parallel and series to reach a required capacity and voltage. The states of battery cells, e.g., voltage, SoC, and state of health (SoH), are regulated by the battery management system (BMS). Thirdly, the load profile of PPL is simplified. In this Ph.D. project, the study on PPL is based on a square wave profile, while the pulsed power's rising and falling take some time in practice. Furthermore, the load profile of PPLs could be a triangle wave or other more complicated shape, which depends on the load type and operation scenario. PPL profiles may require different control considerations and affect the PPS circuit parameter design.

1.4. THESIS OUTLINE

The thesis consists of two parts: **Report** and **Selected publications**. The report structure and contents of each chapter with corresponding publications are shown in Table 1-2. Summaries of each chapter are as follows:

- **Chapter 1. Introduction**
  Introduction of the research background, motivation, and limitations of this Ph.D. project are clarified.
- **Chapter 2. Investigation of MVDC SMGs**

Table 1-2. Report structure and related publications for each chapter.

Chapter No.	Contents	Relevant Publications
1	Introduction	J2, J3, J4
2	Investigation of MVDC SMGs	J1, J2
3	SoC balancing method Coordinated control strategy	C1 J3
4	Impact of PPL Control of PPS	C2 J4
5	Conclusions	-

State of the art of hardware and software aspects in MVDC SMGs are reviewed, including the power architecture, power components, control strategies, stability analysis, and protection schemes.

- **Chapter 3. Coordinated control in DC SMGs**
  A coordinated control strategy for generators and battery packs in the DC SMG to achieve stable voltage regulation and power sharing is presented. Besides, the SoC balancing method for battery packs are presented.
- **Chapter 4. Analysis and control of PPS**
  The impacts of the PPL characteristics on the DC SMG are observed. Based on this, the requirements on the PPS are obtained. Then an improved control method based on SMC for the PPS is proposed to achieve stable voltage regulation with fast power tracking. Comparisons with conventional methods demonstrate the effectiveness of the presented method.
- **Chapter 5. Conclusions**
  Throughout this Ph.D. project, all contributions are highlighted, and future work is marked.

1.5. PUBLICATION LIST

The research dissemination of the Ph.D. project includes journal papers and conference publications, as listed in the following.

Journal papers

J1. **L. Xu**, J. Guerrero, A. Lashab, B. Wei, N. Bazmohammadi, J. Vasquez and A. Abusorrah, "A Review of DC Shipboard Microgrids – Part I: Power Architectures, Energy Storage and Power Converters," *IEEE Trans. Power Electron.*, vol. 37, no. 5, pp. 5155-5172, 2022.

J2. **L. Xu**, J. Guerrero, A. Lashab, B. Wei, N. Bazmohammadi, J. Vasquez and A. Abusorrah, "A Review of DC Shipboard Microgrids – Part II: Control Architectures, Stability Analysis and Protection Schemes," *IEEE Trans. Power Electron.*, vol. 37, no. 4, pp. 4105-4120, 2022.

J3. **L. Xu**, B. Wei, Y. Yu, J. Guerrero, and J. Vasquez, "Coordinated Control of Diesel Generators and Batteries in DC Hybrid Electric Shipboard Power System," *Energies*, vol. 14, no. 19, p. 6246, 2021.

J4. **L. Xu**, J. Matas, B. Wei, Y. Yu, Y. Luo, J. Vasquez, and J. Guerrero, " Sliding Mode Control for Pulsed Load Power Supply Converters in DC Shipboard Microgrids," *Int. J. Electr. Power Energy Syst.*, under review, 2022.

Conference Papers

C1. **L. Xu**, B. Wei, J. Vasquez, and J. Guerrero, "State of Charge Balance of Distributed Batteries in DC Shipboard Microgrids," in *2nd China International Youth Conference on Electrical Engineering (CIYCEE)*, Chengdu, 2021.

C2. **L. Xu**, B. Wei, Y. Yu, J. Vasquez, and J. Guerrero, "Simulation Assessment of the Impact of Pulsed Loads in DC Shipboard Microgrid," in *Proc. 47th Annual Conference of the IEEE Industrial Electronics Society (IECON)*, Toronto, 2021.

CHAPTER 2. INVESTIGATION OF MVDC SMGS

2.1. INTRODUCTION

The development of power electronics makes it feasible to develop advanced SPSs. Motivated by the environmental protection requirements clarified in section 1.1, the concept of MVDC SMG in advanced electric ships is becoming popular due to its merits compared with AC counterparts [50], such as:

- Reduced fuel consumption by enabling variable-speed SG operation.
- Flexibility in the integration of SGs without the need for phase angle synchronization and other DC sources (e.g., batteries, FCs, and UCs).
- Small footprint with the elimination of the switchgear and 50/60Hz transformer.

An overview of a typical MVDC SMG is depicted in Figure 2-1. All the onboard power components, including functional blocks and power converters, can be arranged in specific system architecture. Since there are numerous power components integrated in the system, and the operation condition in maritime application is harsh, while the system has to be compact and reliable, it is complex to control and manage

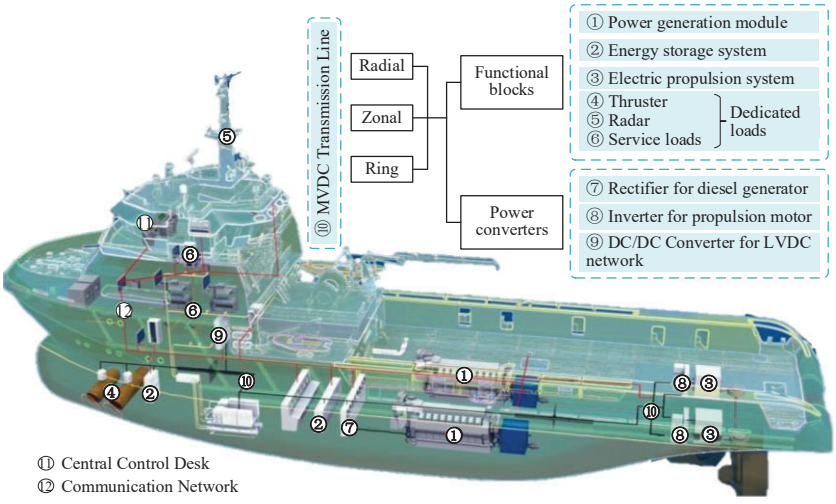

Figure 2-1 Typical MVDC SMG configuration [J1].

the onboard electric equipment. The exploration on MVDC SMGs is still ongoing case by case, and it is necessary to have a comprehensive overview to address the developments in this field by summarizing the features, challenges, and potential research trends in MVDC SMGs.

This chapter reviews the MVDC SMGs from the aspects of hardware configurations and software control issues. System architectures and power components, including typical shipboard functional blocks and power converters, are given in Section 2.2. The control issues of coordinated control strategies, system stability, and protection schemes are discussed in Section 2.3. Section 2.4 presents the summary.

2.2. SYSTEM ARCHITECTURES AND HARDWARE POWER COMPONENTS

The hardware configurations of MVDC SMGs and onboard power components vary by ship type and design requirements. Though the development of MVDC SMGs is still in the early developing stage, there are a few standards to comply with when designing the system and some recommendations on system architecture and voltage level to follow. The functional blocks from which the particularities of SMGs come, including typical power sources, shipboard loads, and ESS, are summarized from research and commercial ship cases. Since it is the trend that SMG capacities increase for larger shipping capability, the power conversion stages through which the functional blocks are integrated into the system in MVDC maritime applications are reviewed.

2.2.1. SYSTEM ARCHITECTURES

Considering requirements on system reliability, operation flexibility, and energy density in different vessels, the system architecture of the SMG should be designed properly. Though there are limited standards specifically for MVDC SMGs up to now, IEEE Std 1709-2010 [31] provides recommendations on the system design, and three main system architectures are mentioned: radial, zonal, and ring architecture, shown in Figure 2-2 (a), (b), and (c), respectively.

1) Radial architecture. It consists of port and starboard MVDC buses that connected through a bus-tie, and the shipboard sources and loads are symmetrically arranged. This framework has been widely implemented till now, since it allows easy retrofit from the conventional mechanical-driven system to modern electric alternatives [18].

2) Zonal architecture. Together with radial one, zonal architecture is also suggested in the IEEE standard, and it has been adopted by the US navy for its high reliability [51]. It features the division of shipboard loads into several power centers,

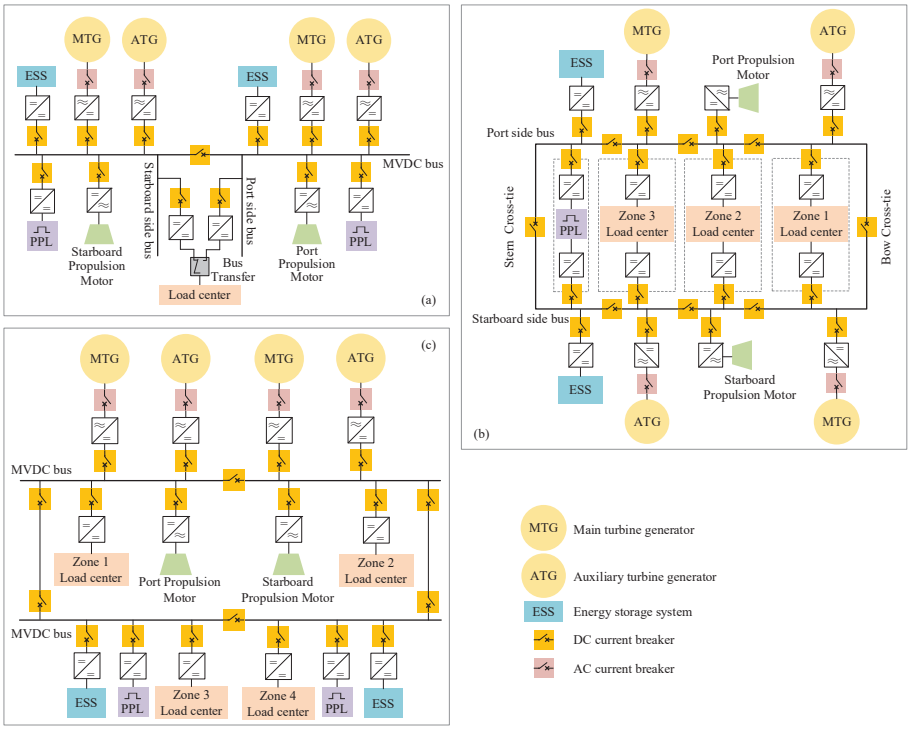

Figure 2-2 System architectures of MVDC SMG [J1].

each of which has two power paths to the MVDC bus as the mutual backup. In military ships, the specific high power PPLs are set isolated from other service loads [31]. In addition to the dual connections in load zones, the longitudinal bus makes it possible to isolate faults with a minimum shutdown area and reduces the cable cost.

3) Ring architecture. It can be seen as an 'intermediate version' between radial and zonal frameworks, as two MVDC buses are connected and form a loop, while the electric components connect to the bus in an order similar to the radial scheme. The ring architecture is rarely adopted in newly built SMGs.

Qualitative comparisons among the above three architectures in terms of bus scheme, reliability, survivability, reconfigurability, complexity, and popularity are clarified in publication [J1] in detail. In summary, the radial architecture requires the least breakers and holds the worst overall performance on the above measurements. In contrast, the zonal architecture has the best performance in the cost of system complexity with more breakers needed, especially in cases with long bus loops. Thus, design suggestions on system architecture can be concluded that small ships with few components and do not require high reliability can choose radial bus architecture,

while ships with high needs on reliability and survivability suit zonal architecture better.

2.2.2. FUNCTIONAL BLOCKS

According to the electrical components onboard, function blocks are categorized as power generation module (PGM), ESS, electric propulsion system, and dedicated high power loads. Here, the functional blocks refer to the equipment devoted to specific functions, while the associated power converters are discussed in the following subsection.

1) PGMs. At present, diesel generators are still the primary PGMs in most ships, and FCs are becoming popular in research for maritime applications. For all-electric ships, batteries are the only power sources, and a detailed description on battery will be given in the ESS part.

In the catalog of diesel generators, the marine generation module, consisting of prime mover and SG, converts the chemical energy in diesel or heavy fuel oil to mechanical energy, then to electric energy [52]. Gas turbines are also adopted in the applications, such as naval vessels and auxiliary gen-sets in industrial ships, which require high efficiency and wide speed range [53]. For the SGs, wound-rotor synchronous motor (WRSM) and permanent-magnet synchronous motor (PMSM) are the most common types in market, and these two generator types have similar performance in output capability.

The alternative of SGs in ships can be FCs, which convert chemical energy in fuels to electrical energy by chemical reaction by different techniques instead of burning, such as alkaline FC, direct methanol FC, proton exchange membrane FC, and solid oxide FC [25]. Thus, it is possible to achieve emission-free and improve efficiency. Fuels such as methanol, hydrogen, and liquid natural gas are applicable for FCs in different operation conditions and design considerations. FCs have the benefits of a long lifetime, while the dynamic response is relatively slow due to the internal electrochemical and thermodynamic reactions [54].

2) ESS. The shipboard ESS enables a more efficient and flexible operation by coordinating with the PGMs [55]. Available techniques include battery ESS (BESS), UCs, FESS, and superconducting magnetic ESS (SMESS) [27]. Among these, there are significant differences in characteristics, as shown in Table 2-1. BESS has a relatively high energy rating due to its scalability, making it possible to act as the backup energy source and meet long-term demands. In contrast, UC and FESS have a high power range with short response time but relatively small energy rating, indicating they are suitable for providing transient high power to meet short-term load demands. In practice, UC and FESS usually cooperate with BESS to be a HESS so that the merits of each ESS type can be combined [56]. Besides, SMESS is a

Table 2-1. Comparisons of shipboard ESS [J1].

Technique	BESS	UC	FESS	SMESS
Power range	0.9-2 MW	Up to 50 MW	0.03-100 MW	Up to 10 MW
Energy range	0.3-10 MWh	0.02-0.3 MWh	Up to 5 MWh	0.07-5 MWh
Dynamics	Few to 40ms	10-20ms	<=4ms	Milliseconds
Charge time	Tens of minutes to hours	Few to tens of minutes	Few to tens of minutes	Seconds
Discharge time	Minutes to hours	Milliseconds to 1 hour	Up to 15 minutes	Few minutes
Power density	0.05-2 kW/kg	0.5-10 kW/kg	0.4-1.5 kW/kg	Up to 100 kW/kg
Efficiency	60%-80%	>95%	80%-95%	>95%
Cases	MF Herjólfur ferry, AIDAperla cruise	Notional catamaran	Demonstrator electric ship at Alstom	Notional cases

promising technique with a very high efficiency and power density, though it requires a higher cost to maintain the cryogenically cooled condition for superconducting coils [57].

3) Electric propulsion system. In general, propulsion motors take around 80% of the shipboard load demand [52], showing that the propulsion system's performance may affect the system significantly. Typical propulsion motor types include DC motor, induction motor (IM), wound-field synchronous motor (WFSM), permanent magnet synchronous motor (PMSM), and other special motors. DC motors were used in the past due to their flexibility of accurate torque control and speed control. However, DC motors need maintenance due to the wear and tear of commutators, and brushless DC motors have increased size and weight [58]. In comparison, AC machines gain much attention with reduced maintenance costs and a simplified structure. IMs feature the benefits of solid robustness and long lifetime but require a large starting current, and multi-phase IMs can be implemented for high power ratings [59]. WFSMs are slightly more efficient than IMs [60], and there is no power limitation. PMSMs are more advanced without an excitation system and, therefore, more efficient and compact. But it has safety problems if a fault occurs while the motor is always excited [60]. Besides, motors adopting superconducting technique are developed for ship application. Detailed comparisons among these motor types can be found in publication [J1]. In summary, WFSM and PMSM have the benefits in power range and efficiency, and IM is superior in reliability and cost. Other motor types only take up a tiny fraction of the practical cases.

4) Dedicated high power loads. Aside from electric propulsion motors, several other onboard high-power loads are fed from the MVDC bus, e.g., bow and stern thrusters and air conditioning compressors. While some service loads, communication systems, auxiliaries, and electronics are supplied by the LVDC bus. Additionally, in

naval ships, weapon loads, e.g., electromagnetic aircraft launch system (EMALS) and pulsed radar, consuming high pulsed power are a particular load type and need dedicated design considerations [61].

2.2.3. POWER CONVERTERS

Power converters are the interfaces of functional blocks to the SMG. According to the aimed functionality, three main types of power converters in MVDC SMGs are rectifiers interfacing generators and the MVDC bus, inverters interfacing propulsion motors and the MVDC bus, and DC/DC converters connecting ESS and LVDC to the MVDC bus. Compared with electric vehicle applications, power converters in electric ships should have higher power and voltage ratings and higher reliability. Besides, general requirements on power density, efficiency, and cost are also desired.

1) Rectifier. The rectifier on the generator side converts the generator terminal voltage to the MVDC bus voltage. Suitable topologies for this application include the two-level rectifier and multilevel rectifier. In the two-level category, the switches can be diode, thyristor, or IGBT [62]. Diode rectifiers can satisfy the voltage conversion need of unidirectional power flow from the generator to the DC network. Additionally, the diode switches are simple, reliable, and cheap. The DC bus voltage is regulated by generator excitation control and speed control if using diode rectifiers, as clarified in section 1.1.2. It is possible to scale up the voltage and power ratings by having multiple diode two-level rectifiers in the terminal of the multiphase generator, as shown in Figure 2-3 (a). Alternatives of diode switches are thyristor and IGBT switches, with which the two-level rectifiers could have voltage with good power quality [63]. Modular multilevel converter (MMC) that is popular in high voltage DC (HVDC) power systems could also be an option for MVDC ships to meet future higher power demands and obtain better fault tolerance [64]. Figure 2-3 (b) shows the MMC rectifier topology with N submodules (SMs) in each arm. The cascaded half-bridge and full-bridge SMs bring the converter voltage scalability, redundancy, and reduced voltage stress on switches, but it has the drawback of bulky size and weight [65], [66].

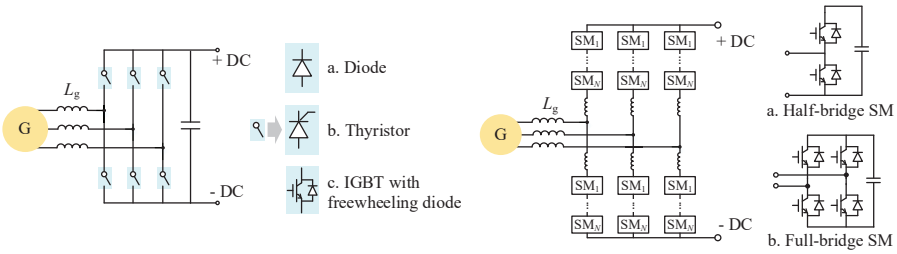

Figure 2-3 Topologies of rectifiers for onboard generators [J1].

Table 2-2. Comparisons of rectifiers and inverters topologies [J1].

	Diode rectifier*	Thyristor rectifier / LCI	IGBT rectifier*	MMC		NPC**	ANPC**
				Half-bridge	Full-bridge		
Output voltage levels	-	-	2	N+1		3	
Voltage stress		v_{dc}		v_{dc} /N		v_{dc} /2	
Filter Inductor size		High		Low		Medium	
Capacitor number		1		6N		2	
Switching frequency	-	10^0-10^1 kHz		10^{-1} kHz		10^{-1}-10^0 kHz	
Number of switches	6 diodes	6 thyristors	6 IGBTs	12N IGBTs	24N IGBTs	12 IGBTs and 6 diodes	18 IGBTs
Control complexity	No control needed	Simple		Complex		Medium	
Fault tolerance		×		√		×	
Fault ride-through capability		×		×	√	×	

Comparisons of rectifier topologies are shown in Table 2-2. Two-level rectifiers have merits of compactness and high reliability with less switches than MMCs, while MMCs have better fault management ability. Therefore, small or short-distance ships with limited space could choose two-level rectifiers for good reliability and economy. While for large vessels requiring a high power supply and operating in harsh conditions, MMC rectifiers can provide a reliable solution.

2) Inverter. The inverters together with the variable frequency drives enable flexible and efficient operation of propulsion motors. The inverters on the propulsion motor side should meet the motor capacity and have a high voltage ramp, low harmonics, and low losses [67]. Among typical inverter topologies for ship electric propulsion, neutral point clamped (NPC) inverters and MMC, shown in Figure 2-4 (b) and (c) respectively, are broadly available in commercial vessels. Nevertheless, two-level load-commutated inverter (LCI), as shown in Figure 2-4 (a), is widely used for synchronous motor speed control [68]. Similar to two-level rectifiers, multiphase configurations based on the two-level topology can be structured for higher voltage ratings [69]. Three-level NPC has the benefits of lower semiconductor stresses and better power quality than the two-level topology and simpler circuit than multilevel topologies. Active NPC (ANPC) replaces the clamping diode in NPC with the active controllable switch to solve the problem of unsymmetrical temperature distribution of semiconductor junction [70]. There are mature products based on above topologies for marine propulsion drive in the market.

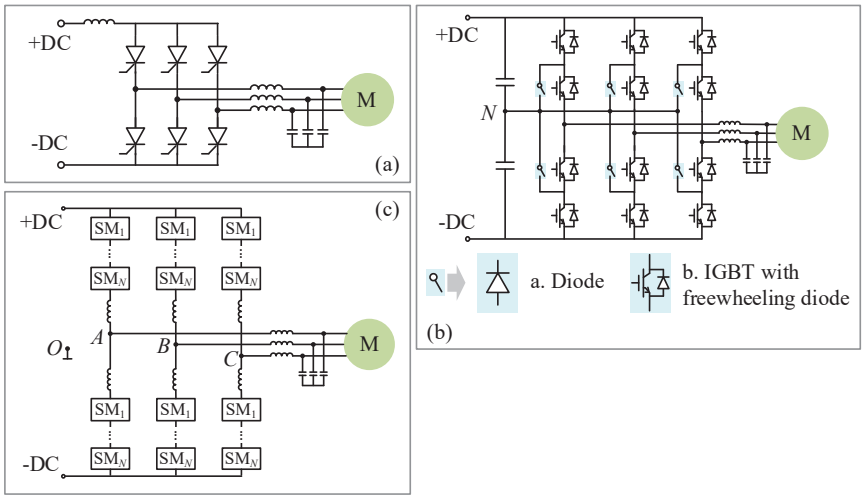

Figure 2-4 Inverter topologies for shipboard propulsion motors [J1].

Comparisons among four potential inverter topologies are shown in Table 2-2. It can be concluded that the two-level inverter has benefits in power density and reliability, while MMC has higher control flexibility. NPC and AMPC have medium performances in terms of switch stress, converter size, and control performance. Topology selection suggestions are that big ships with high power demand on propulsion can choose the multi-level inverters with flexible control performance at the more considerable size cost, while two-level inverters fit small ships.

3) DC/DC converter. DC/DC converters discussed in this section include the interfaces between the MVDC buses and the ESSs as well as the LVDC buses. DC/DC converters with galvanic isolation are preferred in medium voltage applications. Figure 2-5 (a)-(c) show three topologies used in marine application: input-series-output-parallel (ISOP) dual active bridge (DAB) DC/DC converter [71], NPC-based DC/DC converter [72], and isolated MMC DC/DC converter (iM2DC) [73]. In these

Table 2-3. Comparisons of DC/DC converter topologies [J1].

	ISOP DAB	iM2DC		NPC-based DC/DC converter
		Half bridge	Full bridge	
Voltage stress	v_{dc}/N and v_{dc}	v_{dc}/N		$v_{dc}/2$ and v_{dc}
Inductor and transformer number	N transformers	12 inductors and one transformer		One transformer
Capacitor number	$2N$	$12N$		3
Switching frequency	10^{-1}-10^{0} kHz	10^{-1}-10^{0} kHz		10^{-1} kHz
Number of switches	$8N$	$16N$	$32N$	10
Control complexity	High	High		Medium
Fault tolerance	×	√		×
Fault ride-through capability	√	×	√	×

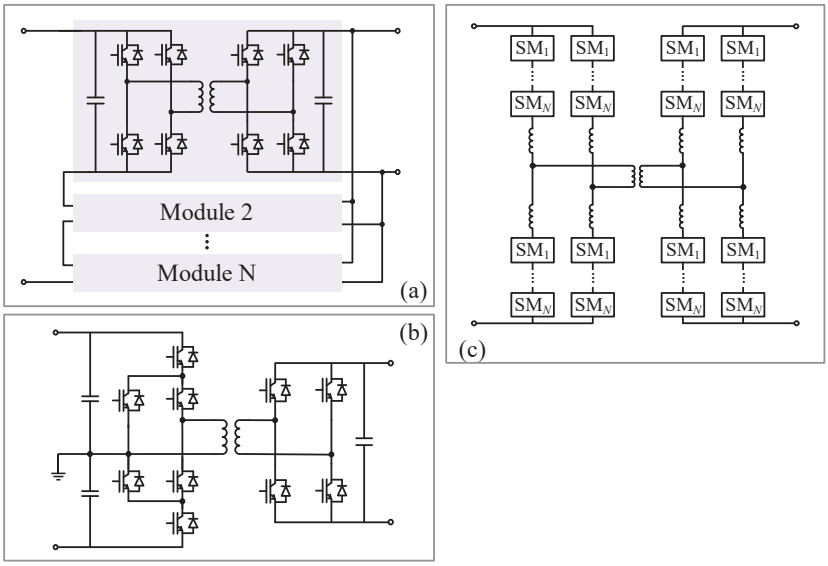

Figure 2-5 DC/DC converter topologies in DC SMGs [J1].

topologies, high frequency transformers are used for voltage step-up/down and galvanic isolation for personal safety with small size. Comparisons among these three topologies are shown in Table 2-3. They all fit for high-power applications and are capable of managing faults. Especially, NPC-based DC/DC converter is relatively simple and requires fewer passive components than the other two topologies, while ISOP DAB and iM2DC, with the modular structure, are fault tolerant, which is preferred in ships.

2.3. CONTROL STRATEGIES, STABILITY, AND PROTECTION

Technical assessments of an SMG can be taken from the aspects of reliability, energy efficiency, maneuverability, and so on. The SMG is vulnerable to disturbances since it operates without support from the main grid. Remarkably, the operation conditions and load profile in naval ships are much harsher than in industrial vessels, leading to a higher demand on system survivability to resist attacks and failures [74]. Hence, the goal of designing the SMG control system is to ensure power supply reliability, system stability and survivability at minimal additional costs.

2.3.1. CONTROL STRATEGIES

The overall objectives of the control system are to provide the shipboard loads with a stable and reliable power supply and to ensure the power sources are working at an efficient operating point. Thus, the shipboard functional blocks' characteristics must be considered when designing the controllers. The control configuration in DC

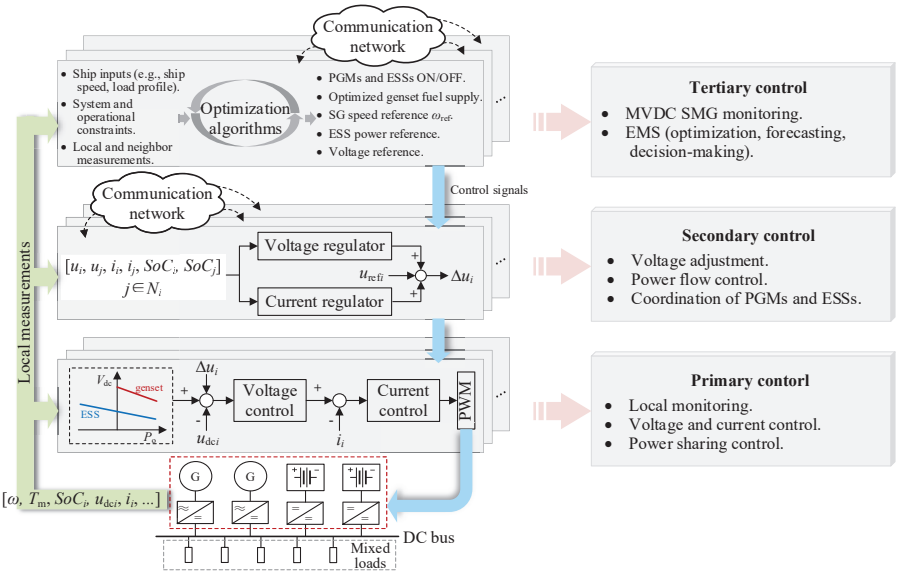

Figure 2-6 Block diagram of hierarchical control in DC SMGs [J2].

SMGs can be referred from terrestrial DC microgrids, and the hierarchical control has been approved to be effective in SMG application [75]. Figure 2-6 shows the overall scheme of hierarchical control in DC SMGs. The primary control focuses on sharing the load among PGMs and ESS taking the sources' characteristics into consideration [41], the secondary control aims at the bus voltage regulation, and the tertiary control consists of an EMS, in which different optimization objectives can be achieved considering system constraints [76]. According to the requirement of the communication network, the hierarchical control can be achieved in a centralized, decentralized, or distributed manner [77].

The commands generated at the high control level, such as voltage references and power setpoints of each PGM and ESS, are sent to the following lower-level controllers. At the tertiary level, multi-objective EMS can be implemented to optimize the overall operation. Typical optimization objectives include fuel consumption minimization [78], operation cost minimization [79], and power loss minimization [80]. In addition to generation side optimization, load management is also a vital part of the tertiary level controller, especially when system faults occur. It is because SMGs' primary load management objective is to ensure the system is stable and avoid overloading sources rather than achieve economical operation like in terrestrial microgrids. The secondary and primary level control configurations are discussed in section 1.1.2.

2.3.2. STABILITY ANALYSIS

The stability issues in DC SMGs come from three aspects: 1) The constant power load (CPL) behavior from power electronic converters, e.g., the propulsion motor drives, 2) The change of operating point when the high-power pulsed power load (PPL) is activated, and 3) The change of operating point when the system is reconfigured.

1) Stability analysis on CPLs.

The CPLs that consume constant power regardless of the input voltage may induce stability degradation due to the negative incremental impedance, which is expressed as:

$$R_{\mathrm{CPL}} = \frac{\partial v_o}{\partial i_o}\Big|_{(V_0, I_0)} = -\frac{P_{\mathrm{CPL}}}{I_0^2} \tag{2.1}$$

where v_o and i_o are the instantaneous voltage and current of the CPL, P_{CPL} is the CPL power at the steady-state operating point (V_o, I_o). The shipboard loads with tightly regulated power converters are the typical CPLs [81].

The simplified circuit model of a n-source DC SMG is shown in Figure 2-7 [82], [83], in which E_k and i_k are the k^{th} (k=1, …, n) output voltage and current of power source side converter, R_{fk}, and L_{fk} are the resistance and inductance of the LC filter, C_{eq} is the equivalent capacitance of the n capacitors. The dynamic model of the circuit is

$$\begin{cases} C_{\mathrm{eq}} \dfrac{dV}{dt} = \displaystyle\sum_{k=1}^{n} i_k - \frac{P_{CPL}}{V_{\mathrm{o}}} \\ L_{fk} \dfrac{di_k}{dt} = E_k - R_{fk} \cdot i_k - V_{\mathrm{o}} \quad \forall k = 1,...,n \end{cases} \tag{2.2}$$

Use Taylor series expansion to linearize (2.2), and the small signal model can be obtained:

$$\begin{bmatrix} \frac{d\Delta V_o}{dt} \\ \frac{d\Delta i_1}{dt} \\ \frac{d\Delta i_2}{dt} \\ \vdots \\ \frac{d\Delta i_n}{dt} \end{bmatrix} = \begin{bmatrix} \frac{1}{C_{eq}R_{CPL}} & \frac{1}{C_{eq}} & \frac{1}{C_{eq}} & \cdots & \frac{1}{C_{eq}} \\ -\frac{1}{L_{f1}} & -\frac{R_{f1}}{L_{f1}} & 0 & \cdots & 0 \\ -\frac{1}{L_{f2}} & 0 & -\frac{R_{f2}}{L_{f2}} & \cdots & 0 \\ \vdots & \vdots & \vdots & \ddots & \vdots \\ -\frac{1}{L_{fn}} & 0 & 0 & \cdots & -\frac{R_{fn}}{L_{fn}} \end{bmatrix} \cdot \begin{bmatrix} \Delta V_o \\ \Delta i_1 \\ \Delta i_2 \\ \vdots \\ \Delta i_n \end{bmatrix} + \begin{bmatrix} 0 & 0 & 0 & \cdots & 0 \\ 0 & \frac{1}{L_{f1}} & 0 & \cdots & 0 \\ 0 & 0 & \frac{1}{L_{f2}} & \cdots & 0 \\ \vdots & \vdots & \vdots & \ddots & \vdots \\ 0 & 0 & 0 & \cdots & \frac{1}{L_{fn}} \end{bmatrix} \cdot \begin{bmatrix} 0 \\ \Delta E_1 \\ \Delta E_2 \\ \vdots \\ \Delta E_n \end{bmatrix} \tag{2.3}$$

Methods to overcome the CPL instability have been studied a lot. Active damping are an effective method that compensates for the negative impedance of the CPL by emulating a virtual impedance [84]. In addition, linearization via state feedback (LSF) is also adopted by compensating for the CPL nonlinear term and then allowing the linear control method to be implemented to eliminate the instability [82].

2) Stability analysis on PPLs.

The shipboard PPLs have high transient power and significant power ramp rate characteristics, which may derive the operating point from the stable area [85].

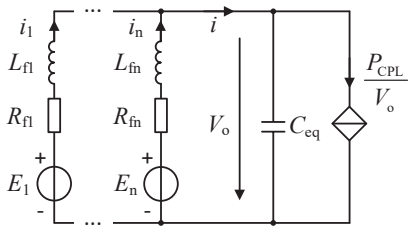

Figure 2-7 Simplified circuit model of the DC SMG [J2].

Therefore, large signal analysis methods are needed to analyze the stability issue induced by PPLs [86]. The analysis can be taken from aspects of studying the system variables in the entire pulse duration period and one single pulse cycle [87]. On the one hand, the system variables have periodic changes since the PPL is activated and inactivated repetitively. In this case, the periodic-orbit analysis method could be suitable for studying the system stability [88]. On the other hand, in view of each pulse cycle, a transient stability analysis is required since the pulsed power presents a large disturbance in the system.

Currently, studies on enhancing stability in the presence of PPLs mainly focus on the management of ESS. In many cases, the HESS consists of UC or FESS together with battery is implemented to meet the power in different frequencies [89]. Besides, proper load shedding is also feasible in generation-demand balancing when PPL works [90].

3) Stability analysis on system architecture.

The system architecture of DC SMGs may have a more significant effect on system stability than that of terrestrial MGs. Since the cable aging in the maritime application is much severer than in land, resulting in line impedance changes, the steady-state operation point may deviate from the initially designed setpoint [91]. Besides, SMGs are more likely to suffer faults, while post-fault reconfiguration may lead to system model changes. Therefore, it is a potential research topic that how to ensure the system stability in case of reconfiguration is activated.

2.3.3. PROTECTION SCHEMES

An SMG's protection system should fulfill fault detection sensibility, selectivity, fault isolation speed, economy, and simplicity [92]. However, there are some barriers to satisfying these demands. As introduced in previous sections, the PPLs absorb large

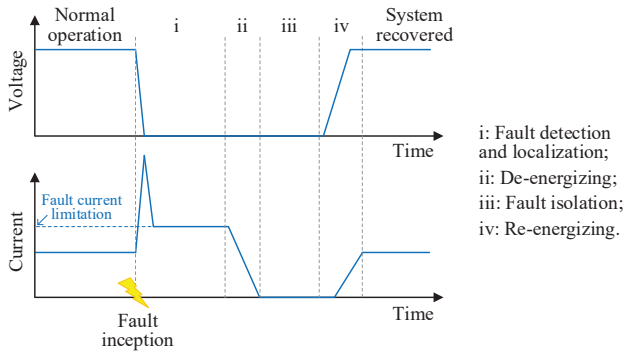

Figure 2-8 Fault management process [J2].

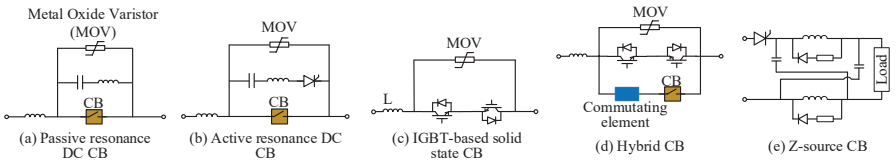

Figure 2-9 Schematics of DC CBs [J2].

transient power; therefore, the current may trigger maloperation of relays and breakers. In addition, grounding systems in ships are difficult to design due to lacking real ground. Current solution takes the hull as the ground, with high resistance or a solidly grounded neutral point [93].

The process of fault management in MVDC SMGs is similar to that in terrestrial MGs. The generic source voltage and current are given in Figure 2-8 [94], and the objective of fault management is to shorten the stage i-iv with accuracy. Methods for each protection process are discussed in this section, and detailed comparisons of techniques in each category can be found in publication [J2].

1) Fault detection and localization.

It is a challenge to detect and localize faults in MVDC SMGs since the presence of PPLs makes it difficult to distinguish fault current and normal pulsed current demand quickly. Furthermore, the small scale of the SMG results in insignificant short-circuit impedance differences in different locations. To detect and localize the faults accurately and speedily, advanced algorithms such as wavelet transform, artificial neural networks, and active impedance estimation may assist in meeting the requirements at the cost of computation burden.

2) Fault isolation.

Once the fault is detected and localized, selected breakers are tripped to isolate the fault. Though it is well known that designing high voltage DC circuit breakers (CBs) is a challenge due to lacking zero-crossing current, several products can meet the demands in part of MVDC and LVDC SMGs in industry [95]. The DC CBs used in SMGs are presented in Figure 2-9. Among these, solid state CBs, hybrid CBs, and Z-source CBs are suitable for high power applications with high safety requirements, at the cost of size and control complexity. While for relatively small SMGs, active resonance DC CBs can meet the basic demands.

3) Post-fault reconfiguration.

To ensure power supply continuity, the post-fault reconfiguration has to be implemented by reconfiguring the bus architecture and implementing load shedding

[96]. In addition to maximizing the power supply coverage, various optimization objectives, e.g., system loss minimization [97] and preserving the stability margin [98], can be designed to reconfigure the system after the fault occurs.

2.4. SUMMARY

This chapter reviews the hardware configuration of MVDC SMGs and associated control issues. Three typical MVDC SMG architectures are presented, and comparisons show that the zonal architecture suits applications requiring high reliability. The shipboard functional blocks include the PGM, ESS, electric propulsion system, and dedicated high power loads. The device types in each category are summarized and compared. Power converters that connect the functional blocks to the system are discussed from the aspects of the converter topologies and power conversion characteristics. In the control aspects, the hierarchical control scheme and the fault management system in DC SMGs are similar to the terrestrial DC MGs. Specifically, the coordinated control between generators and ESS is discussed. Besides, the stability issues in SMGs come from the CPLs, the PPLs, and the system architecture. In terms of fault management, PPLs and the small scale of SMGs make it challenging to detect and locate faults fast and accurately.

Based on publications:

J1. **L. Xu**, J. Guerrero, A. Lashab, B. Wei, N. Bazmohammadi, J. Vasquez and A. Abusorrah, "A Review of DC Shipboard Microgrids – Part I: Power Architectures, Energy Storage and Power Converters," *IEEE Trans. Power Electron.*, vol. 37, no. 5, pp. 5155-5172, 2022.

J2. **L. Xu**, J. Guerrero, A. Lashab, B. Wei, N. Bazmohammadi, J. Vasquez and A. Abusorrah, "A Review of DC Shipboard Microgrids – Part II: Control Architectures, Stability Analysis and Protection Schemes," *IEEE Trans. Power Electron.*, vol. 37, no. 4, pp. 4105-4120, 2022.

CHAPTER 3. COORDINATED CONTROL IN DC SMGS

3.1. INTRODUCTION

Proper coordination of PGMs and ESS for the desired reliability and economy in hybrid electric ships has drawn much attention. The primary goal of the coordination between diesel generators and batteries is to control the bus voltage with acceptable tolerance and have proportional power sharing. With the coordinated control configurations discussed in section 1.1.2 and section 2.3.1, strategies aiming at reducing fuel consumption are usually studied, as the DC system allows the SGs to operate with variable speed according to the load conditions and then reach the optimal specific fuel consumption [38]. [39] discussed the coordination between two variable-speed SGs and one battery in a DC SMG, in which the output power of SGs is set in several power levels to associate with load demands, and the generator rotor speed is given by a lookup table, allowing the SGs to operate with variable speed to some extent. At the same time, the batteries compensate for the power difference. Nevertheless, due to the large inertia in SGs, the dynamic response of speed control would be much slower than the change of load conditions, making the speed optimization has little effect on short-term operation. Moreover, the strategy of reducing the output power of the generator set is not cost-efficient from the aspect of SG sizing. SGs with small power together with BESSs with large capacity provide a solution to overcome this problem. Existing study cases only consider one BESS in the system, while with increasing capacity of the onboard BESS as well as the symmetrical design in zonal architectures, couples of battery packs would be integrated. It is necessary to manage the battery states such as SoC in designing the coordinated control strategies.

This chapter studies a hybrid-electric MVDC SMG having two paralleled diesel generators and two paralleled BESSs. Section 3.2 presents the method to balance SoC between battery packs. In section 3.3, a coordinated control strategy for two SGs and two battery packs is discussed. Then section 3.4 comes to the summary.

3.2. SOC BALANCING METHOD FOR DISTRIBUTED BATTERY PACKS

3.2.1. CONTROL PRINCIPLE

In DC SMGs, the generic droop control involves adjusting the voltage along with the output power, expressed as

$$u_{dci}^{*} = U_{dc}^{*} - m_i \cdot P_{oi} \tag{3.1}$$

where u_{dci}^{*}, m_i, and P_{oi} are the voltage reference, the droop coefficient, and the output power of the i^{th} converter respectively, and U_{dc}^{*} is the voltage reference at idle load.

For the battery packs under droop control, the battery SoC can be implemented in the droop control configuration and achieve the SoC balance by adjusting the droop coefficient. In the proposed method, the droop coefficient for the discharging and charging mode is defined as:

$$m_i = \begin{cases} m_d \cdot \left(1 - \mathrm{SoC}_i\right)^n & \text{Discharging} \\ m_c \cdot \mathrm{SoC}_i^n & \text{Charing} \end{cases} \tag{3.2}$$

where m_d and m_c are the maximum droop coefficient in discharging and charging mode respectively, SoC_i is the SoC of i^{th} battery pack, and n ($n > 0$) is the adjustment coefficient. According to the voltage tolerance limit, ±10% at the steady state in DC SMGs [31], m_d and m_c can be determined by the maximum discharging power P_{d_max} and maximum charging power P_{c_max} as follows:

$$\begin{aligned} m_d &\le \frac{U_{dc}^{*} \times 10\%}{P_{d\_\max}} \\ m_c &\le \frac{U_{dc}^{*} \times 10\%}{P_{\mathrm{c}\_\max}} \end{aligned} \tag{3.3}$$

Neglecting the line impedance in the SMG, the output voltage of each converter equals to the point of common coupling (PCC) voltage u_{dc}. Then the ratio of output power in each battery pack follows:

$$P_{o1} : \cdots : P_{oi} = \begin{cases} \dfrac{1}{\left(1-\mathrm{SoC}_1\right)^n} : \cdots : \dfrac{1}{\left(1-\mathrm{SoC}_i\right)^n} & \text{Discharging} \\ \dfrac{1}{\mathrm{SoC}_1^n} : \cdots : \dfrac{1}{\mathrm{SoC}_i^n} & \text{Charging} \end{cases} \tag{3.4}$$

The battery packs with high SoC discharge in higher current, therefore reducing the SoC faster and vice versa, reaching SoC balance in the end.

Use the Coulomb counting method to calculate the battery SoC, which is expressed by

$$\mathrm{SoC}_i(t) = \mathrm{SoC}_i(t=0) - \frac{1}{C_{ei}u_{bi}}\int p_{oi}dt \tag{3.5}$$

in which C_{ei}, u_{bi}, and p_{oi} are the capacity, voltage, and power of the i^{th} battery pack, respectively. Take (3.4) into (3.5), the SoC change in the i^{th} battery pack is derived:

$$\mathrm{SoC}_i(t) = \begin{cases} \mathrm{SoC}_i(t=0) - \dfrac{p_{bat}}{C_{ei}u_{bi}}\displaystyle\int \frac{1/(1-\mathrm{SoC}_i)^n}{\sum 1/(1-\mathrm{SoC}_i)^n}dt & \text{Discharging} \\ \mathrm{SoC}_i(t=0) - \dfrac{p_{bat}}{C_{ei}u_{bi}}\displaystyle\int \frac{\mathrm{SoC}_i^{\,n}}{\sum \mathrm{SoC}_i^{\,n}}dt & \text{Charging} \end{cases} \tag{3.6}$$

where p_{bat} is the total required power from the battery packs.

A case study of two paralleled battery packs with the initial SoC of 0.4 and 0.6 is tested in discharging and charging modes. The numerical solution of (3.6) is shown in Figure 3-1. The results verify the presented method and show that higher coefficient n leads to faster balancing.

3.2.2. STABILITY ANALYSIS

For the purpose of evaluating the stability of the proposed method, a small signal method is used. During the discharging process, combining (3.1) and (3.2), and having the disturbances in the variables, it can be obtained as:

$$\Delta u_{dci} = m_d n(1-\mathrm{SoC}_i)^{n-1} i_{oi}\Delta\mathrm{SoC}_i - m_d(1-\mathrm{SoC}_i)^n \Delta i_{oi} \tag{3.7}$$

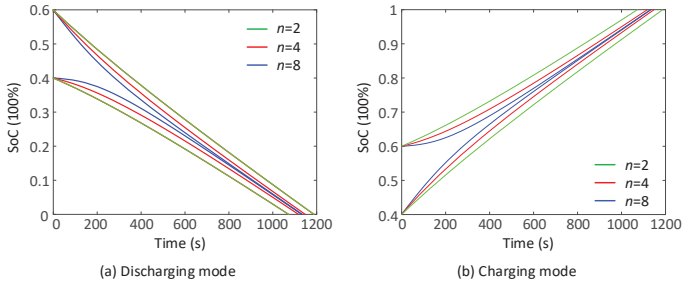

Figure 3-1 Numerical solution of battery SoC [C1].

Use a first-order low pass filter (LPF) in the power sampling as follows:

$$P_{oi} = G_{LPF} \cdot p_{oi} = \frac{\omega_c}{s+\omega_c} \cdot p_{oi} \tag{3.8}$$

in which ω_c is the cutoff frequency of the LPF. Perturb (3.5), and combine the result with (3.7), it comes to:

$$\begin{aligned} \Delta P_{oi} &= -\frac{\lambda_i \Delta u_{dci}}{m_d \left(1-\mathrm{SoC}_i\right)^{n-1}\left[nP_{oi}+\lambda_i\left(1-\mathrm{SoC}_i\right)\right]} \\ \lambda_i &= sC_{ei}u_{bi}G_{LPF} \end{aligned} \tag{3.9}$$

Meanwhile, small signal expression in the load side can be expressed as:

$$\Delta p_{load} = \frac{2u_{dc}\Delta u_{dc}}{R_{load}} \tag{3.10}$$

where p_{load} and R_{load} are the power and resistance of the load, and u_{dc} is the PCC voltage, which equals to the output voltage of converters when neglecting the line impedance. With power matching in the battery side and load side, it yields:

$$\sum_{i=1}^{N} \frac{\lambda_i}{-m_d \left(1-\mathrm{SoC}_i\right)^{n-1}\left[nP_{oi}+\lambda_i\left(1-\mathrm{SoC}_i\right)\right]} = \frac{2u_{dc}G_{LPF}}{R_{load}} \tag{3.11}$$

As an example, consider a system consisting of two batteries with the same parameters ($C_{e1} = C_{e2} = C_e$, $u_{b1} = u_{b2} = u_b$). The characteristic equation is obtained:

$$As^3 + Bs^2 + Cs + D = 0 \tag{3.12}$$

where,

$$A = \left(1-\mathrm{SoC}_1\right)^{n-1} nP_{o1} + \left(1-\mathrm{SoC}_1\right)^{n} C_e u_b \omega_c + \left(1-\mathrm{SoC}_2\right)^{n-1} nP_{o2} + \left(1-\mathrm{SoC}_2\right)^{n} C_e u_b \omega_c$$

$$\begin{aligned} B = {} & 2\omega_c n\left(1-\mathrm{SoC}_1\right)^{n-1} P_{o1} + \omega_c^2\left(1-\mathrm{SoC}_1\right)^{n} C_e u_b + 2\omega_c n\left(1-\mathrm{SoC}_2\right)^{n-1} P_{o2} + \omega_c^2\left(1-\mathrm{SoC}_2\right)^{n} C_e u_b \\ & + \frac{2m_d u_{dc} n^2}{C_e u_b R_{load}}\left(1-\mathrm{SoC}_1\right)^{n-1}\left(1-\mathrm{SoC}_2\right)^{n-1} P_{o1}P_{o2} + \frac{2m_d u_{dc} n\omega_c}{R_{load}}\left(1-\mathrm{SoC}_1\right)^{n}\left(1-\mathrm{SoC}_2\right)^{n-1} P_{o2} \\ & + \frac{2m_d u_{dc} n\omega_c}{R_{load}}\left(1-\mathrm{SoC}_1\right)^{n-1}\left(1-\mathrm{SoC}_2\right)^{n} P_{o1} + \frac{2m_d u_{dc}\omega_c^2 C_e u_b}{R_{load}}\left(1-\mathrm{SoC}_1\right)^{n}\left(1-\mathrm{SoC}_2\right)^{n} \end{aligned}$$

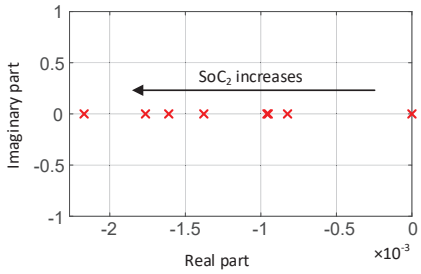

Figure 3-2 Dominant poles of the proposed battery pack SoC balancing method [C1].

$$C=\omega_c^2 n\left(1-\mathrm{SoC}_1\right)^{n-1}P_{o1}+\omega_c^2 n\left(1-\mathrm{SoC}_2\right)^{n-1}P_{o2}+\frac{4m_d u_{dc}\omega_c n^2}{C_e u_b R_{load}}\left(1-\mathrm{SoC}_1\right)^{n-1}\left(1-\mathrm{SoC}_2\right)^{n-1}P_{o1}P_{o2}$$
$$+\frac{2m_d u_{dc}\omega_c^2 n}{R_{load}}\left(1-\mathrm{SoC}_1\right)^{n}\left(1-\mathrm{SoC}_2\right)^{n-1}P_{o2}+\frac{2m_d u_{dc}\omega_c^2 n}{R_{load}}\left(1-\mathrm{SoC}_1\right)^{n-1}\left(1-\mathrm{SoC}_2\right)^{n}P_{o1}$$

$$D=\frac{2m_d u_{dc}\omega_c^2 n^2}{C_e u_b R_{load}}\left(1-\mathrm{SoC}_1\right)^{n-1}\left(1-\mathrm{SoC}_2\right)^{n-1}P_{o1}P_{o2}$$

The system dominant poles are obtained through the characteristic equation, as shown in Figure 3-2. Without losing generality, keep SoC_1 constant and change SoC_2 from 0 to 1. It can be found that the dominant poles locate in the left half of s domain, indicating the system is stable. The stability analysis of the charging process is similar, and it has been verified in [99].

3.3. COORDINATED CONTROL FOR HYBRID-ELECTRIC DC SHIPS

A coordinated control for a DC SMG with two diesel generators, two BESSs, and mixed shipboard loads is presented in this section. The system configuration is shown in Figure 3-3.

The proposed coordinated control aims to achieve efficient and flexible operation in various load conditions. The shipboard diesel generators are desired to maximize their utilization by allowing them to provide energy intensively and efficiently. In practice, SGs reach the highest fuel efficiency when the load factor is in the range of 80-90%, as an example of a shipboard SG efficiency curve is shown in Figure 3-4 [100]. Thus, it is reasonable to set the generator power in a certain range and let the battery packs regulate the power balance between SGs and loads in various load conditions.

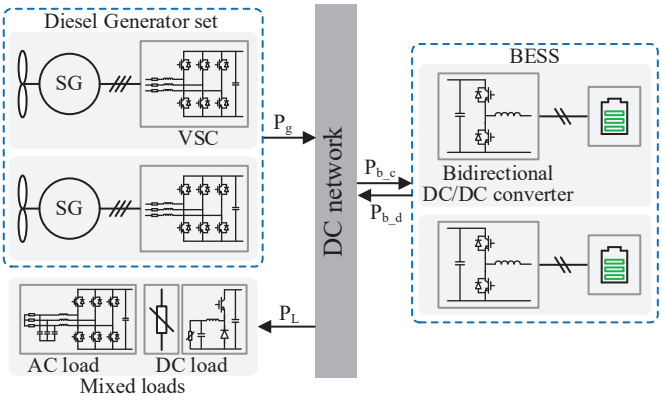

Figure 3-3 Configuration of the studied DC SMG [J3].

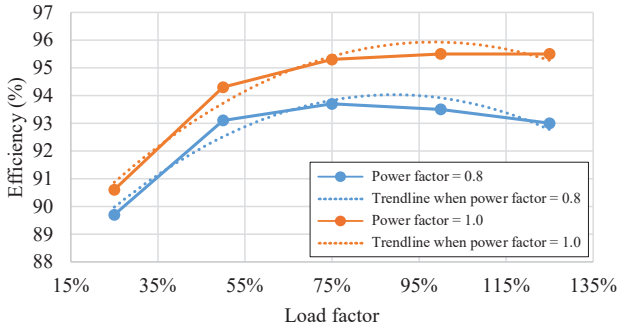

Figure 3-4 SG efficiency versus load factor[100].

Therefore, the coordination principle of the proposed method is to set two operation modes according to the shipboard load conditions and battery states. When the SGs are needed, they are set to provide constant power and operate at the setpoint with the highest efficiency, and the BESSs operate flexibly in charging and discharging states depending on the operation mode. Otherwise, the BESSs supply for the loads independently. The operation mode switching criteria is derived in Figure 3-5.

The two defined operation modes are:

- All-electric mode, suits light load conditions and short voyages, of which the power and energy demands can be fed only by the BESSs. In addition, when the ship berths at the dock and get charged from onshore girds, the all-electric mode is activated to supply the shipboard service loads.

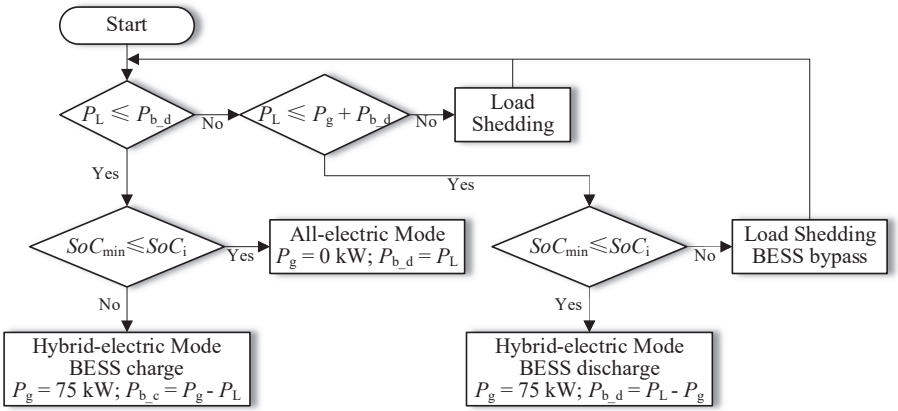

Figure 3-5 Flowchart of operation mode switching.

- Hybrid-electric mode, which suits heavy load conditions, allows diesel generators and BESSs to be integrated into the system. The BESSs discharge and charge to compensate for the power unbalance between generators and loads, allowing the diesel generators to operate at the highest efficiency.

3.3.1. POWER SHARING METHOD

The coordinated control objectives include controlling the bus voltage with acceptable tolerance in various operation conditions and sharing the load between generators and BESSs according to the designed strategy. To achieve this, the control strategies in each operation mode and for flexible mode switching are designed as follows.

On the BESS side, the bidirectional DC/DC converters are responsible for voltage regulation. As the BESSs are integrated in both operation modes, covering the entire ship operation, the SoC of battery packs would change in a wide range. Thus, the battery pack SoC is considered in the primary control to share the power, and meanwhile the SoC can be balanced to extend the battery lifetime. A secondary control regulating the voltage adjustment. The generated voltage reference is expressed by (3.13).

$$
\begin{aligned}
u_{dci}^{*} &= U_{dc}^{*} - R_{dbi} \cdot i_{bi} + \Delta\delta_{bi} \\
\Delta\delta_{bi} &= k_{sp} \cdot \left(U_{dc}^{*} - u_{dci}\right) + k_{si} \int \left(U_{dc}^{*} - u_{dci}\right) dt \\
R_{dbi} &= \begin{cases} \dfrac{m_d}{SoC_i^n} & i_{bi} > 0 \\ m_c \cdot SoC_i^n & i_{bi} < 0 \end{cases}
\end{aligned}
\tag{3.13}
$$

where u_{dci}^{*}, R_{dbi}, and u_{dci} are the voltage reference, the droop coefficient, and the output voltage of the i^{th} converter, i_{bi} and SoC_i are the output current and SoC of the i^{th} battery pack, U_{dc}^{*} is the voltage reference at idle load, k_{sp} and k_{si} are the control parameters in the secondary controller, m_d and m_c are the maximum droop coefficient in discharging ($i_{bi} > 0$) and charging ($i_{bi} < 0$) mode respectively, and n ($n > 0$) is the adjustment coefficient.

The control scheme is depicted in Figure 3-6. The SoC-based droop coefficient regulation allows the battery pack with high SoC to discharge in larger current, making the SoC reduces faster and vice versa, reaching SoC balance eventually. Therefore, over-discharging and overcharging in one single battery pack can be avoided.

On the SG side, the generators are controlled to operate at the efficient setpoint, outputting 80% of the rated power. A dual loop consisting of the power loop and current loop is implemented to achieve the constant power control in the active rectifier, as the block diagram depicted in Figure 3-7. Here, to operate at unity power factor, the reactive power reference is set to zero.

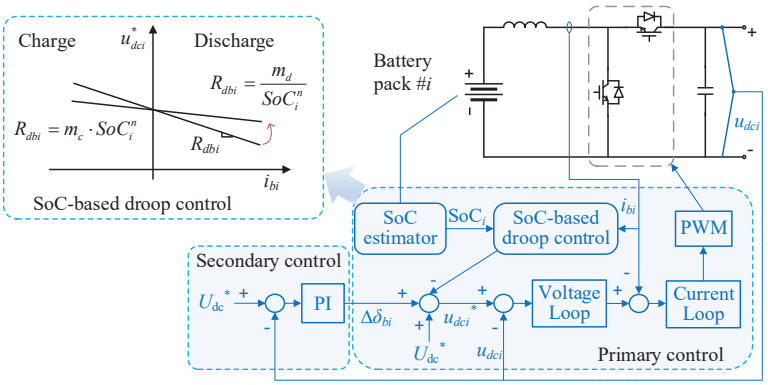

Figure 3-6 Control scheme of BESS side converter [J3].

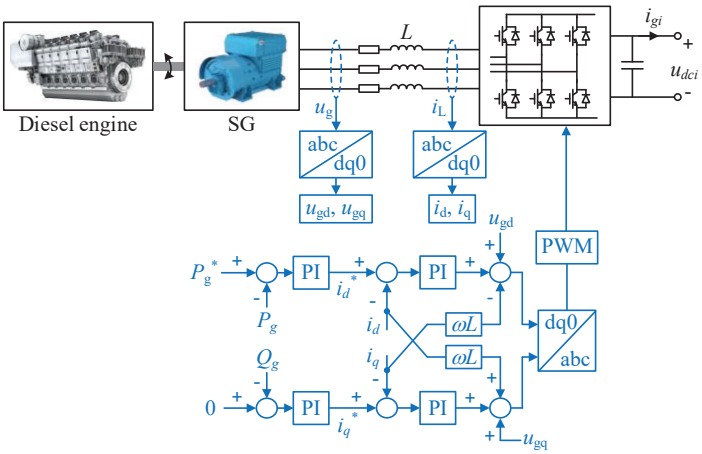

Figure 3-7 Control scheme of SG side converter [J3].

3.3.2. SIMULATION RESULTS

A notional 1kV MVDC SMG is simulated based on Matlab/Simulink to test the proposed coordinated control method. The circuit and control parameters are given in Table 3-1.

Table 3-1. Circuit and control parameters of the MVDC SMG [J3].

Categories	Parameters	Values
MVDC bus	Rated voltage	1 kV (±10%)
BESS	Rated voltage	600 V
	Rated capacity	50 Ah
	Rated discharging current	100 A
	Rated charging current	50 A
	Initial SoC of two BESSs	40% and 60%
Bidirectional DC/DC converter and associated controller	Inductance	1 mH
	DC-link capacitance	2 mF
	Switching frequency	20 kHz
	Current controller K_{dpi}, K_{dii}	0.6, 20
	Voltage controller K_{dpv}, K_{div}	0.78, 300
	Secondary controller K_{sp}, K_{si}	0.01, 30
	Coefficient m_{disc}	0.05
	Coefficient m_{ch}	0.2

SG	Rated power	93.75 kW
	Nominal line-to-line voltage (RMS)	440 V
	Nominal frequency	50 Hz
	d-axis synchronous reactance (X_d)	0.875 p.u.
	d-axis transient reactance (X'_d)	0.19 p.u.
	d-axis subtransient reactance (X''_d)	0.136 p.u.
	q-axis synchronous reactance (X_q)	0.1625 p.u.
	q-axis subtransient reactance (X''_q)	0.135 p.u.
	Stator leakage reactance (X_l)	0.0163 p.u.
	d-axis transient time constant (T'_{do})	0.31 s
	d-axis subtransient time constant (T''_{do})	0.027 s
	q-axis subtransient time constant (T''_q)	0.01 s
Rectifier and associated controller	DC-link capacitance	3 mF
	Synchronous inductance	1.7 mH
	Inductor resistance	0.07 Ω
	Switching frequency	20 kHz
	Current controller K_{rpi}, K_{rii}	2, 200
	Power controller K_{rpv}, K_{riv}	1, 100

Scenario 1: all-electric mode. This operation mode is activated when the BESSs are capable of supplying for the load demand independently. The load consumption is 100kW, 120kW, and 80kW at t = 0, 20s, and 40s.

The simulation results are demonstrated below. The DC bus voltage fluctuation during load changes is controlled within tolerance, as shown in Figure 3-8. The BESS 1 with low initial SoC discharges with a smaller current than the BESS 2 with higher

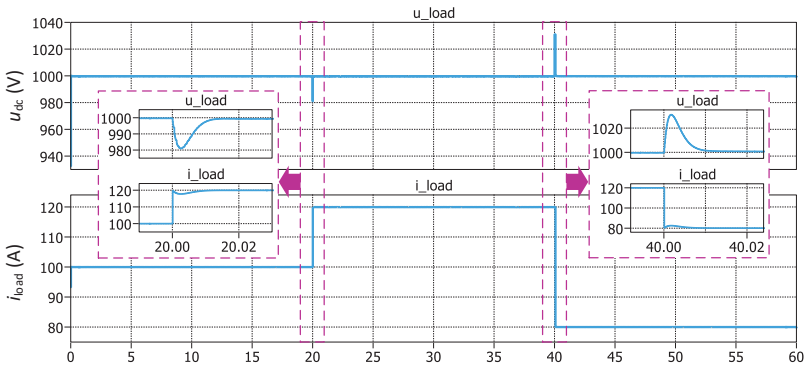

Figure 3-8 The DC bus voltage and load current in scenario 1 [J3].

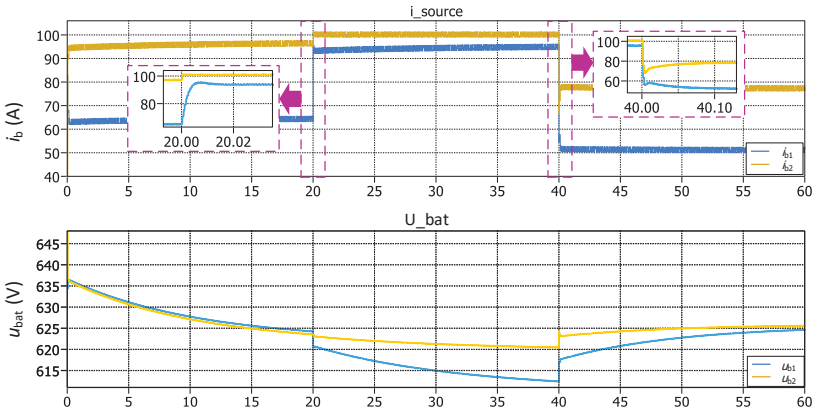

Figure 3-9 Current and voltage of BESS in scenario 1 [J3].

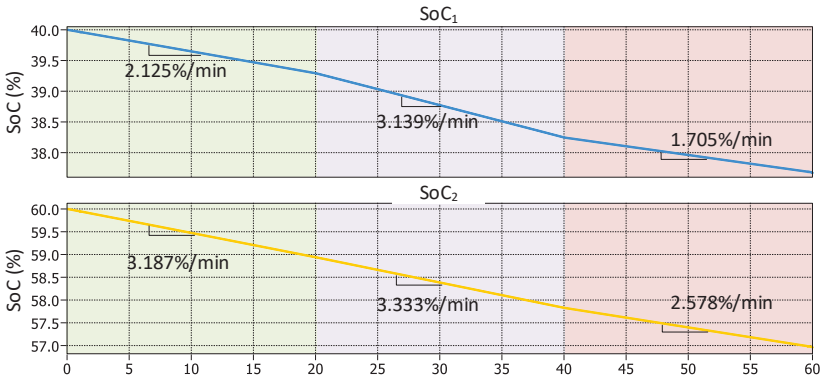

Figure 3-10 Two BESSs' SoC in scenario 1 [J3].

initial SoC, as shown in Figure 3-9, and the trend of SoC change is presented in Figure 3-10. The current sharing ratio follows the ratio of SoC between two BESSs.

Scenario 2: hybrid-electric mode. Both charging and discharging states of the BESSs are included in this operation mode. The load changes from 100kW to 200kW at t = 20s, requiring the BESSs to shift from charging to discharging. The simulation results of bus voltage, SG and BESS current, and SoC are presented from Figure 3-11 to Figure 3-13, respectively. The rectifiers output constant current regardless of load conditions, and the power difference is compensated by the two BESSs as designed. BESS 1 with a smaller initial SoC gets charged with a larger current and discharges less current than BESS 2 with a higher initial SoC.

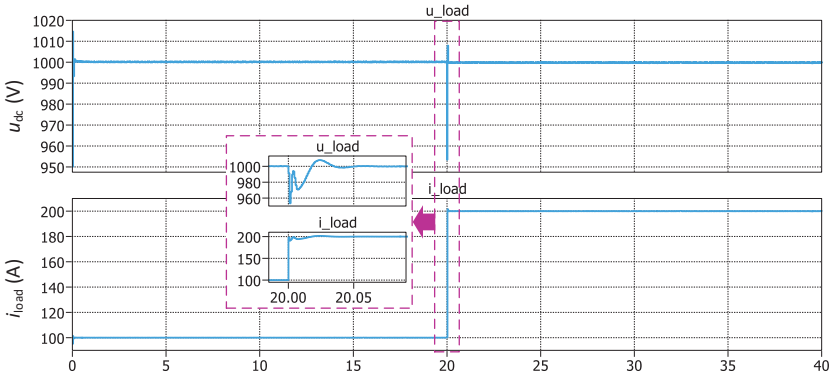

Figure 3-11 The DC bus voltage and load current in scenario 2 [J3].

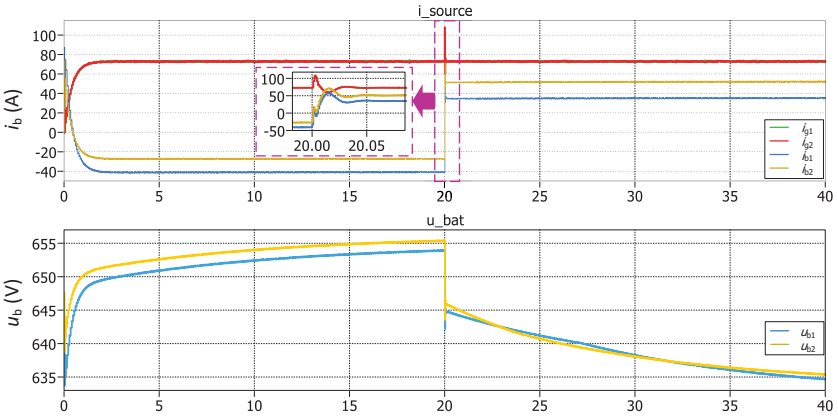

Figure 3-12 Current and voltage of BESS in scenario 2 [J3].

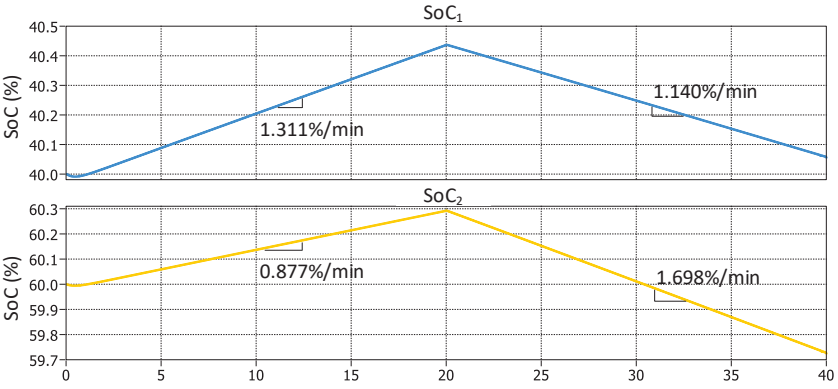

Figure 3-13 Two BESSs' SoC in scenario 2 [J3].

Scenario 3: mode shifting. The shift between the previously defined two modes is tested, under the conditions of from all-electric mode, hybrid-mode and BESSs charging, hybrid-mode and BESS discharging, and back to all-electric mode. Simulation results are shown in the following. The DC bus voltage in Figure 3-14 shows the voltage fluctuation during mode switching is within the tolerance of ±10% of the rated value. The current sharing in each operation mode and different load conditions shown in Figure 3-15 follows the designed rules, and the associated changes of BESS SoC are shown in Figure 3-16.

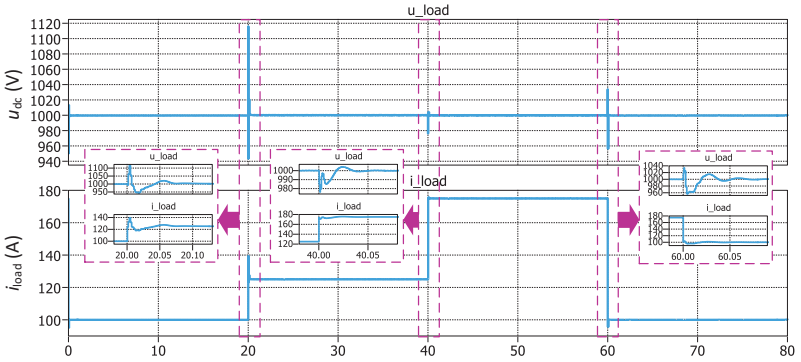

Figure 3-14 The DC bus voltage and load current in scenario 3 [J3].

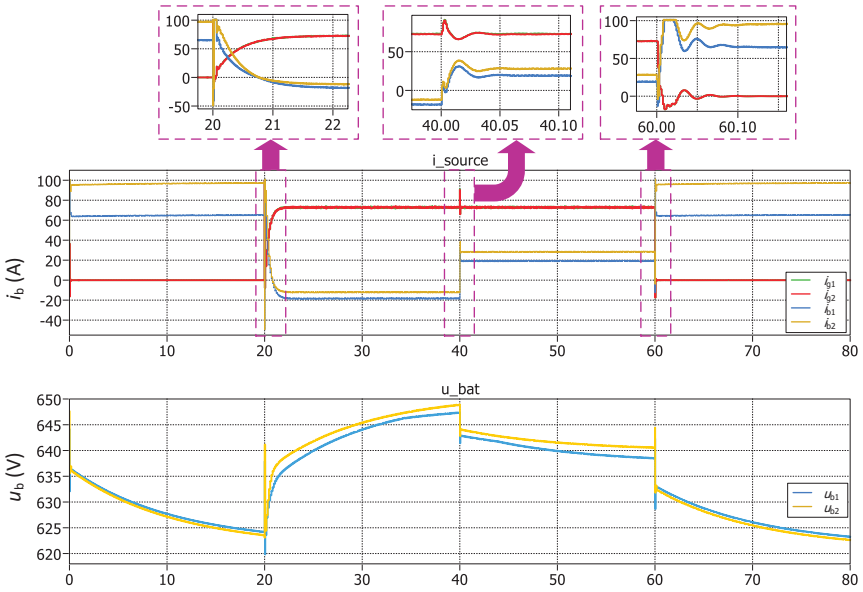

Figure 3-15 Current and voltage of BESS in scenario 3 [J3].

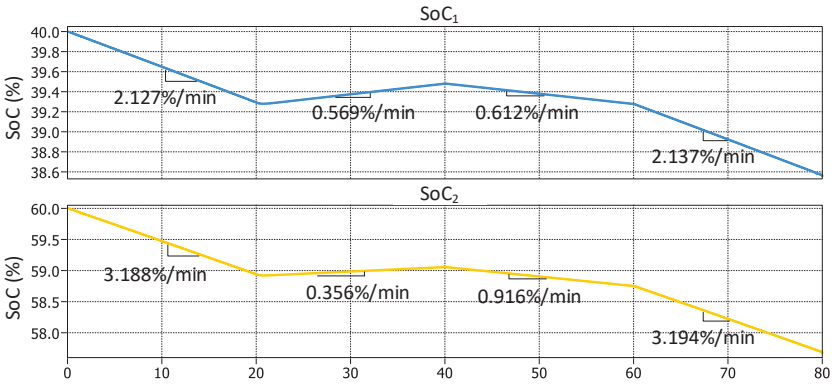

Figure 3-16 Two BESSs' SoC in scenario 3 [J3].

3.4. SUMMARY

This chapter delivers a coordinated control strategy between SGs and BESSs in a MVDC hybrid-electric ship to achieve efficient and flexible operation. Two operation modes are designed according to the potential load conditions, and smooth mode switching can be obtained under the proposed control strategy. Besides, SoC balance between the BESSs can be obtained with this controller. The coordinated control is achieved by implementing constant power control realized by the rectifiers in the SG side to have efficient generator operation and SoC-based droop control in the BESS side to control the DC bus voltage. Simulation results show the effectiveness of the coordinated control method in various load conditions, and a smooth shift between all-electric and hybrid-electric operation modes can be achieved.

Based on publications:

C1. **L. Xu**, B. Wei, J. Vasquez, and J. Guerrero, "State of Charge Balance of Distributed Batteries in DC Shipboard Microgrids," in *2nd China International Youth Conference on Electrical Engineering (CIYCEE)*, Chengdu, 2021.

J3. **L. Xu**, B. Wei, Y. Yu, J. Guerrero, and J. Vasquez, "Coordinated Control of Diesel Generators and Batteries in DC Hybrid Electric Shipboard Power System," *Energies*, vol. 14, no. 19, p. 6246, 2021.

CHAPTER 4. ANALYSIS AND CONTROL OF PPS

4.1. INTRODUCTION

The load profile in advanced electric ships is sophisticated due to the changeable navigation and operation conditions. Especially in military vessels, the high-power weapons and sensors, such as electromagnetic railgun and pulse radar, draw pulsed power in high pulse repetition frequency (PRF), therefore usually being seen as PPLs [45], [101]. The presence of PPLs in ships with limited generation capacity may lead to a bus voltage drop and further affect other onboard electric loads [102]. Thus, supplying the shipboard PPLs has challenges in system design and control to ensure the system is stable and efficient. PPLs have mainly been studied from the perspective of how to mitigate their adverse impact through ESS management [43], [47]. Generally, UCs and FESSs, which have high power density and are capable of discharge in fast response, are good options to supply PPLs. In these solutions, the energy storage units are directly connected to the PPL in parallel, therefore, requiring the capacity of the ESS to be equal to or even higher than the load demand, which is not cost-efficient. Instead, using an active capacitor converter [103] or a two-stage configuration [104] to provide the pulsed power to the PPL can reduce the need for the storage capacitor and thus reduce the cost. However, these methods are based on the conventional PI control, which is fit for the linearized systems, while it may have problems for systems with PPLs since the significant load fluctuation may cause a change of the system operating point. In such cases, nonlinear control methods are preferred. SMC may fit the PPS application due to its benefits in fast dynamics and robustness to perturbations [105].

In this chapter, the impacts of different parameters of PPLs on system voltage are studied, and based on this, an improved method based on SMC for the PPS is presented to achieve the goal of supplying the PPLs with fast power tracking and economical configuration. Section 4.2 presents the modeling of PPLs, and the impacts of different PPL parameters on bus voltage are investigated. In section 4.3, the control method for the PPS is clarified, and an improved method with fast dynamics and robustness is implemented. Section 4.4 gives the summary.

4.2. MODELING AND ANALYSIS ON PPLS

4.2.1. MODELING OF PPLS

The profile of PPLs features intermittent pulses with a pulse duration t_p and pulse interval time Δt in the peak power of P_p. Usually, there are several pulse cycles in one operation, and the entire pulse duration is referred to as t_{ep}. The load profile varies from PPL types, of which some examples are given in Table 4-1. In one pulsed cycle T_p, the power profile of a PPL can be expressed as:

$$p_p(t) = \begin{cases} P_p, & t_0 < t \le t_0 + t_p \\ 0, & t_0 + t_p < t \le T_p \end{cases} \tag{4.1}$$

Table 4-1. Parameters of typical PPLs in ships [C2].

PPL type	P_p (MW)	t_p (ms)	Δt (s)	t_{ep} (s)
EMALS	~10^2	~10^0	~10^1	~10^1
Rail gun	~10^3	10^{-1}-10^0	~10^0	10^0-10^1
Pulsed radar	~10^1	10^{-1}-10^0	~10^0	10^0-10^1

Generic PPL circuit is modeled by a small resistor with a switch that modifies the connection state of PPL or by a controlled current source [106], and a storage capacitor parallel connects to the PPL acting as the energy buffer.

4.2.2. IMPACTS OF PPLS ON DC BUS VOLTAGE

A time-domain simulation study on the impacts of different PPL parameters is taken to obtain a complete understanding of their impacts on system voltage performance. In the case of P_{pmax} being less than the generation power, the pulsed power demand can be referred to as load disturbances, and the effect of the PPL can be seen as acceptable load changes in the system. However, the situations would be different if P_{pmax} exceeds the system generation power, in which case the PPL parameters may affect the voltage control performance significantly. This section therefore examines the simulation assessment of the conditions where PPL demand exceeds the system generation. A study of a 200kW pulsed signal with three pulses in a 150kW system is tested.

1) Pulse duration t_p. Keep the pulse period T_p constantly as 10ms and increase t_p from 0.5ms to 50ms. Figure 4-1 shows associated DC voltage changes. It can be found

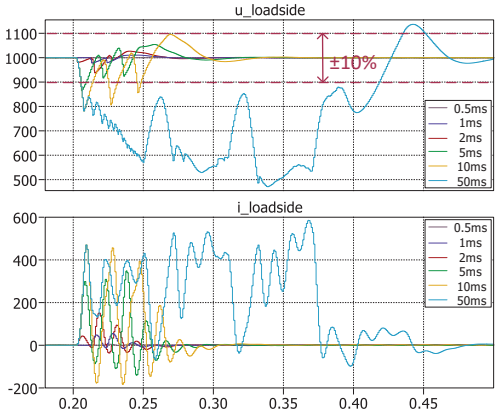

Figure 4-1 DC bus voltage and current with varying t_p [C2].

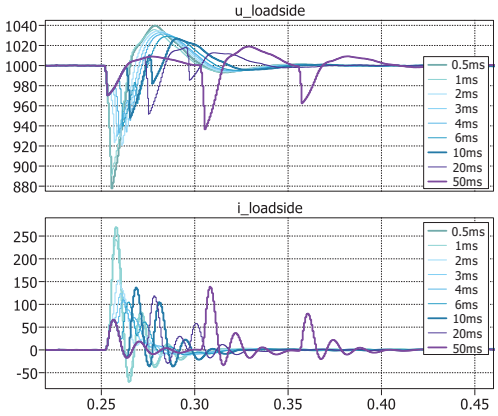

Figure 4-2 DC bus voltage and current with varying Δt [C2].

that the voltage sag is small when t_p is short, while when t_p is much longer than Δt, meaning the duty cycle of the pulsed signal is close to 1, the voltage sag is large, and the voltage stability is significantly affected.

2) Pulse interval time Δt. Keep the pulse duration t_p constant as 2ms and increase Δt from 0.5ms to 50ms. Corresponding DC bus voltage changes are shown in Figure 4-2. It can be found that short Δt, equivalent to the duty cycle is close to 1, makes the pulsed signal having the effect of a signal with long pulse duration, therefore resulting in large voltage sag. While when Δt is long compared with t_p, the voltage sag caused

by each pulse has the similar maximum voltage deviation, which can be found in the cases of Δt = 10ms, 20ms, and 50ms.

3) Entire pulse duration t_{ep}, which can also be represented by pulse number. From previous simulation results, the DC bus voltage deviation at a given peak power depends on the relation between t_p and Δt. When t_p and the pulse duty cycle are small enough, the voltage fluctuation can be relatively small and repeat periodically with the same number of pulses. Otherwise, long t_{ep} leads to severe voltage drop since the effect of each pulse accumulates in the next pulse cycle.

In summary, for the PPL which exceeds the system generation power, the caused voltage drop relates to the t_p, Δt and t_{ep}. Long t_p and short Δt bring a significant voltage drop. PPLs with multiple pulses with small pulse duty cycles produces the voltage drop similar to the effect of each single pulse signal, while a large pulse duty cycle would lead to a severe voltage deviation and long t_{ep} make the system out of voltage stability. These results may help in designing the system generation capacity to achieve economy.

4.3. SLIDING MODE CONTROL FOR PPS

In last section, the impact of PPLs on the DC bus voltage is evaluated, and it can be found the pulsed power demand causes severe voltage fluctuation that may affect the operation of other shipboard loads. This section focuses on the method to mitigate the negative impact of PPLs and provide a reliable power supply to the PPL.

4.3.1. PULSED POWER SUPPLY USING ACTIVE CAPACITOR CONVERTER

The system configuration of a notional MVDC SMG is shown in Figure 4-3, in which the PPS consists of a DC/DC converter as the interface to the MVDC bus, an

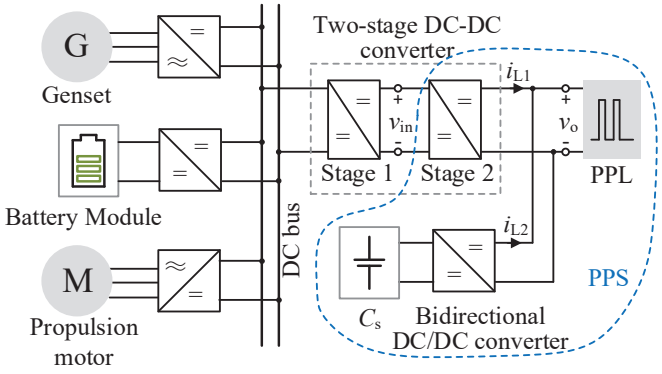

Figure 4-3 Configuration of a MVDC SMG with a PPS [J4].

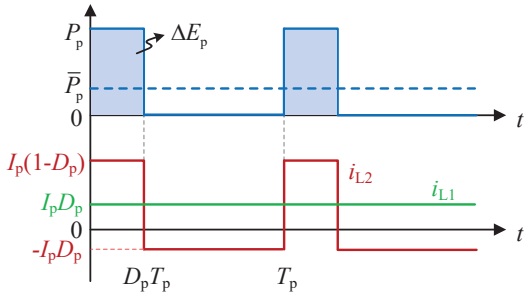

Figure 4-4 PPL profile and the ideal waveforms of the power suppliers [J4].

active-controlled capacitor C_s, and the PPL. The 1kV MVDC bus voltage is stepped down by the two-stage DC/DC converter to 200V and then to 24V in the PPL.

Aiming to mitigate the DC bus voltage fluctuation, the control principle of the PPS is designed as follows. The DC bus feeds the PPS with a constant power that equals the average power of the PPL, and the pulsed power component in the load profile is provided by the active capacitor, as shown in Figure 4-4, in which ΔE_p is the incremental energy in one pulse cycle T_p, D_p is the pulse duty cycle, and P_p is the peak power of the PPL.

The circuit of the PPS is shown in Figure 4-5 (a). The sizing of the passive components should fulfill the energy demand according to the coordination principle between the active capacitor and the SMG-side converters.

1) The storage capacitor C_s. In one pulse cycle, the energy C_s discharged during $[0, D_pT_P]$ equals to the charged energy during $[D_pT_P, T_P]$, and the voltage ripple on C_s

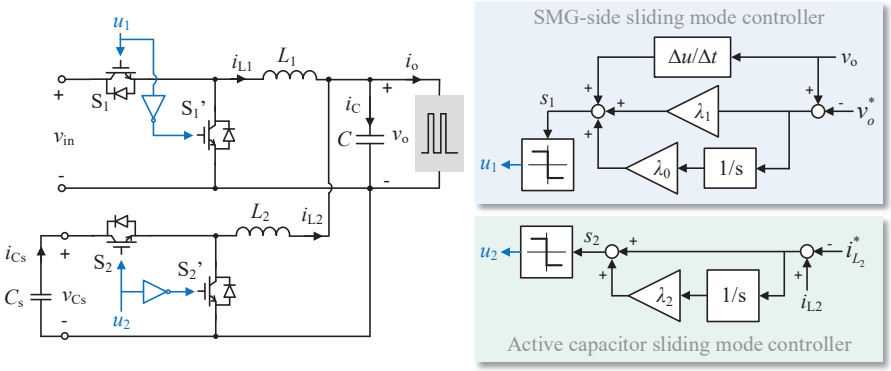

(a) PPS circuit (b) Control diagram of the PPS

Figure 4-5 Diagram of PPS circuit and controllers [J4].

is constrained that the minimum voltage of C_s is higher than the load voltage to ensure the buck converter is working. Thus, the capacitance of C_s can be obtained as:

$$C_s = \frac{\left(1-D_p\right)P_p D_p T_p}{\Delta v_{Cs} \cdot \bar{v}_{Cs}} \tag{4.2}$$

in which, Δv_{Cs} and $\bar{v}_{Cs}$ are the voltage ripple and the average voltage of C_s.

2) The SMG-side inductor L_1. In one switching cycle of the converter, the current ripple in L_1 can be calculated by either the switch S_1 being ON or OFF states, in which the voltage on L_1 is v_{L1_ON} and v_{L1_OFF}, respectively.

$$\begin{aligned}\left|i_{L1\_\min} - i_{L1\_\max}\right| &= \frac{v_{L1\_ON}}{L_1} \cdot t_{ON} = \frac{v_{in}-v_o}{L_1} \cdot \frac{D}{f_{\text{sw}}} \\ &= \frac{v_{L1\_OFF}}{L_1} \cdot t_{OFF} = \frac{v_o}{L_1} \cdot \frac{1-D}{f_{\text{sw}}}\end{aligned} \tag{4.3}$$

in which, i_{L1_min} and i_{L1_max} are the minimum and maximum current in i_{L1}, t_{ON} and t_{OFF} are the conducting and cut-off period of the switch S_1, f_{sw} and D are the switching frequency and the duty cycle of the switch S_1. In steady state, i_{L1} is designed to be

$$i_{L1} = \frac{1}{2}\left(i_{L_1\_\max} + i_{L_1\_\min}\right) = D_p \cdot \frac{P_p}{v_o} \tag{4.4}$$

Combining (4.3) and (4.4), the inductance of L_1 can be obtained:

$$L_1 = \frac{v_o\left(v_{in}-v_o\right)}{2v_{in}\alpha i_{L1} f_{\text{sw}}} \tag{4.5}$$

where $\alpha(\times 100\%)$ is the percentage of the allowed ripple current in i_{L1}.

3) The active capacitor converter inductor L_2. The process of deriving L_2 is similar to that of L_1. Note that the aim of the active capacitor is to track the pulsed power quickly, leading to a tradeoff between the current ripple and the current increasing slope in L_2 design. The calculation of L_2 can be derived by (4.5) by replacing i_{L1} with i_{L2}, which in one pulse cycle is

$$i_{L2}=\begin{cases}\left(1-D_p\right)\cdot\dfrac{P_p}{v_o}, & \left[0, D_pT_p\right]\\ 0, & \left[D_pT_p, T_p\right]\end{cases} \tag{4.6}$$

4) The filter capacitor C. As the inductor current increasing slop is limited, the filter capacitor compensates for the transient power difference, resulting in the load voltage fluctuation. In the pulsed power raising period, the duty cycles of two converters are 1, and the load current increases linearly till the desired load current. The relation between the desired load current I_p and current raising time t_r is expressed as

$$I_p=t_r\left[\frac{v_{in}}{L_1}+\frac{\overline{v}_{C_s}}{L_2}-\frac{\left(L_1+L_2\right)\left(v_o^*-\dfrac{1}{2}\Delta v_o\right)}{L_1L_2}\right] \tag{4.7}$$

in which $\overline{v}_{Cs}$ is the initial voltage of C_s, v_o^* is the rated output voltage, and Δv_o is the allowed voltage drop.

During $[0, t_r]$, the voltage drop on C can be calculated by the discharging current and discharging time, and the maximum voltage drop can be calculated as

$$\Delta v_o=\frac{I_p}{2C}t_r \tag{4.8}$$

Then the capacitance can be obtained:

$$C=\frac{I_p^2L_1L_2}{2\Delta v_o\left[L_1\overline{v}_{C_s}+L_2v_{in}-\left(L_1+L_2\right)\left(v_o^*-\dfrac{1}{2}\Delta v_o\right)\right]} \tag{4.9}$$

4.3.2. SLIDING MODE CONTROLLER FOR THE PPS

According to the control principle presented in the last section, the SMG-side converter regulates the output voltage, and the bidirectional active capacitor converter tracks the pulsed power. Thus, the direct voltage control (DVC) and current control based on SMC are adopted respectively to fulfill the control objectives. Both converters use the buck converter topology. Here, the input voltage in the SMG-side

converter is supposed to be well regulated at a constant value by the stage 1 converter in Figure 4-3.

The sliding surface s_1 in the SMG-side converter is designed as (4.10), and the control law u_1 is (4.11) to adjust the output voltage v_o to the reference v_o^*, which is constantly 24V.

$$s_1 = \frac{de_v}{dt} + \lambda_1 \cdot e_v + \lambda_0 \cdot \int e_v \cdot dt \tag{4.10}$$

$$u_1 = \frac{1}{2}\left[1 - sign\left(s_1\right)\right] = \begin{cases} 1, & s_1 < 0 \\ 0, & s_1 > 0 \end{cases} \tag{4.11}$$

in which $e_v = v_o - v_o^*$ is defined as the voltage error, λ_1 and λ_0 are positive coefficients.

Achieving Lyapunov stability and convergent e_v to the sliding surface $s_1 = 0$ in finite time, the derivative of Lyapunov function (4.12) should be negative.

$$V_1\left(s\right) = \frac{1}{2} s_1^2 \tag{4.12}$$

In the active capacitor converter, the sliding surface s_2 is designed as (4.13), and the control law u_2 as (4.14) to regulate the current i_{L2} to track the reference i_{L2}^*, which is calculated by (4.15).

$$s_2 = e_i + \lambda_2 \cdot \int e_i \cdot dt \tag{4.13}$$

$$u_2 = \frac{1}{2}\left[1 - sign\left(s_2\right)\right] = \begin{cases} 1, & s_2 < 0 \\ 0, & s_2 > 0 \end{cases} \tag{4.14}$$

$$i_{L_2}^* = \frac{p_p\left(t\right)}{v_o} - i_{L_1} = \frac{p_p\left(t\right) - D_p P_p}{v_o} \tag{4.15}$$

in which $e_i = i_{L2} - i_{L2}^*$ is defined as the current error, and λ_2 is the positive coefficient.

The overall schematic diagram of the designed controllers is shown in Figure 4-5 (b).

4.3.3. SIMULATION RESULTS

Comparisons are conducted between the improved and conventional controllers to evaluate their effectiveness in terms of dynamic response and measurement noise robustness. A study case involves a 4kW PPL with 15 pulses is simulated, represented by a controlled current source. The calculated circuit and the control parameters are given in Table 4-2. Here, the conventional method is based on a dual-loop controller in the SMG-side converter and a current loop control in the active capacitor, both of which use the basic PI control. Localized LPF is added to the controlled feedback variables in each converter with a cutoff frequency of 100kHz. The control parameters of the PI controllers are tuned to achieve as fast dynamics as possible.

The simulation results under the two control methods are shown in Fig. 4-6. Comparisons in terms of dynamic response and robustness to measurement noise can be found in Fig. 4-6 (a)-(c) and (d)-(f), respectively.

1) Dynamic response.

The dynamic response can be directly observed in the load voltage. Figure 4-6 (a) shows the simulation results of the load current and terminal voltage. Inevitably, voltage fluctuations occur at the starting and terminating of each pulse under both controllers. The voltage can be well controlled within 0.2ms under SMC, while the tradeoff between response time and overshoot in PI control makes the voltage control performances, including the voltage fluctuation and dynamics, worse than the SMC. Figure 4-6 (b) shows the inductor current from the two buck converters and the filter

Table 4-2. PPS circuit and control parameters of SMC and PI controllers.

Circuit parameters			
$\boldsymbol{C_s}$	4.3mF	L_2	2.1 μH
$\boldsymbol{L_1}$	15.8μH	C	1.64mF
$\boldsymbol{v_o^*}$	24V	P_p	4kW
$\boldsymbol{D_p}$	20%	T_p	5ms
$\boldsymbol{v_{in}}$	200V	v_{Cs}	45V
Controller parameters			
SMC controller	SMG-side	$\lambda_0 = 1130^2$, $\lambda_1 = 1.8 \times 10^4$.	
	Active capacitor	$\lambda_2 = 1.2 \times 10^5$.	
PI controller	SMG-side	Voltage loop: $k_{pv} = 75$, $k_{iv} = 10^5$. Current loop: $k_{pi} = 3$, $k_{ii} = 20$.	
	Active capacitor	Current loop: $k_{pi} = 0.08$, $k_{ii} = 50$.	

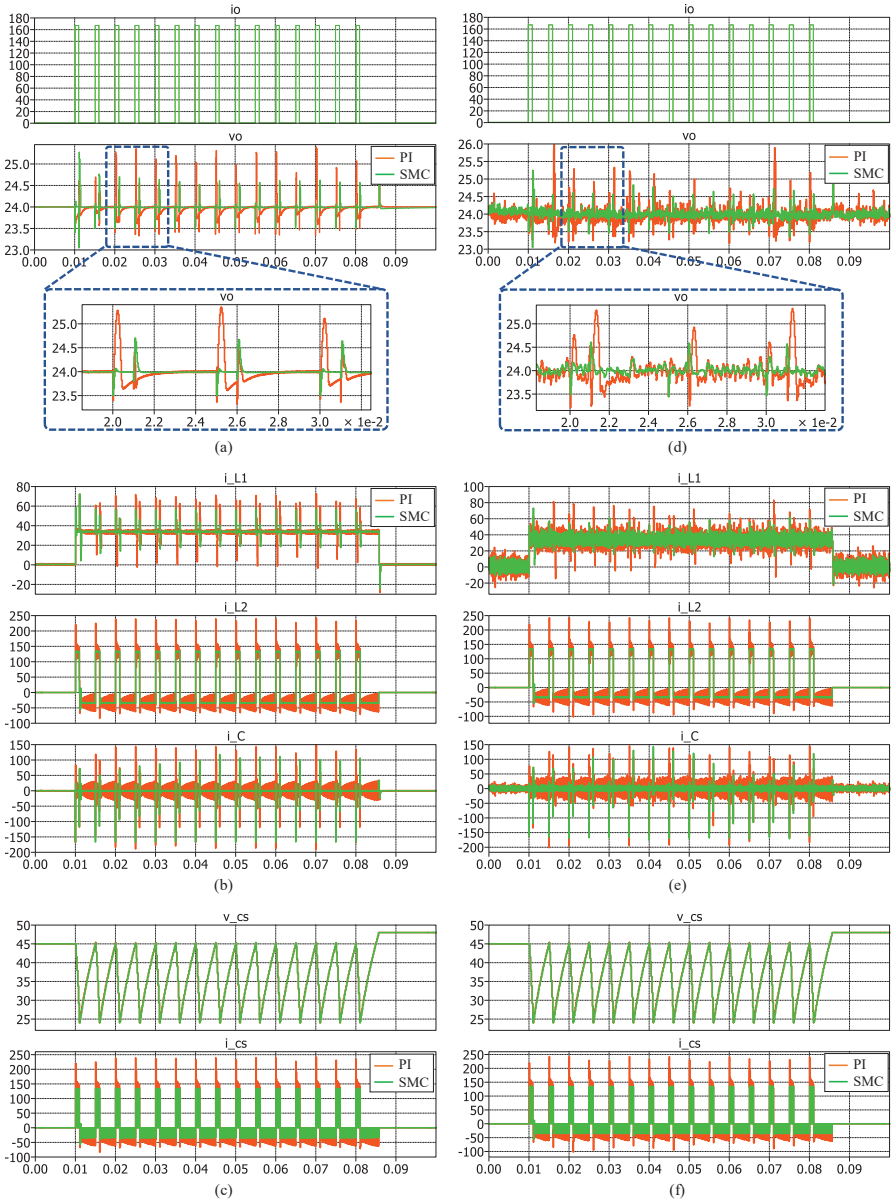

Figure 4-6 Comparative simulation results of the PPS. (a) Load current and load voltage in normal condition. (b) Inductor current and capacitor current in normal condition. (c) Storage capacitor voltage and current in normal condition. (d) Load current and load voltage under measurement noises. (e) Inductor current and capacitor current under measurement noises. (f) Storage capacitor voltage and current under measurement noises.

capacitor current. The current i_{L1} provided by the SMG is controlled to be constantly

34A and has current fluctuations at the raising and falling edges of the PPL pulses. The current i_{L2} tracks the pulsed component in PPL current, and the filter capacitor provides the transient current. It is observed that the current oscillation under SMC-based control is much smaller than using PI control. Storage capacitor C_s voltage and current are shown in Figure 4-6 (c). The initial voltage of C_s is 45V, and C_s deeply discharges and gets charged to the initial voltage at every pulse cycle of the PPL.

2) Robustness.

In order to compare robustness against measurement noises, 1% of the measured parameters' rated values are added as disturbances. The load voltage is shown in Figure 4-6 (d), which shows with the measurement noises, there is an oscillation in the load voltage under both control methods. In comparison, the voltage oscillation under SMC is smaller than that under PI control, indicating that the presented SMC-based method has better robustness to measurement noises. Comparing Figure 4-6 (b) with (d), as well as (c) with (e), both inductor current and storage capacitor current are not significantly affected by measurement noise in the two control methods.

4.4. SUMMARY

This chapter analyses the impacts of PPL profile parameters on the bus voltage and presents an improved method for the PPS based on the SMC. The time-domain simulation revealed that for a PPL with specific peak power, among others, the pulse duration, pulse interval time, and entire pulse duration would affect the voltage stability. Aiming to reduce the adverse impacts of the PPL on system voltage and supply the PPL efficiently, a PPS with the active capacitor is used, and an improved control method based on the SMC is presented. Simulation results verify that the proposed method has faster dynamics in voltage regulation and better robustness against measurement noises.

Based on publications:

C2. **L. Xu**, B. Wei, Y. Yu, J. Vasquez, and J. Guerrero, "Simulation Assessment of the Impact of Pulsed Loads in DC Shipboard Microgrid," in *Proc. 47th Annual Conference of the IEEE Industrial Electronics Society (IECON)*, Toronto, 2021.

J4. **L. Xu**, J. Matas, B. Wei, Y. Yu, Y. Luo, J. Vasquez, and J. Guerrero, " Sliding Mode Control for Pulsed Load Power Supply Converters in DC Shipboard Microgrids," *Int. J. Electr. Power Energy Syst.*, under review, 2022.

CHAPTER 5. CONCLUSIONS

5.1. SUMMARY

This Ph.D. project aims to propose solutions to coordinate the power sources and energy storage units to achieve efficient and reliable system operation. Besides, the particularities of the PPLs in MVDC SMGs are considered, and an improved PPS is presented to address the challenge in power supply for PPLs with mitigated impact on the SMG. The outcomes of this thesis are summarized as follows:

Chapter 1 presents the demands and challenges in developing MVDC SMGs. The concept of MVDC SMGs is developed by targeting green and efficient water transportation. In addition, the shipboard load profiles containing PPLs bring challenges in voltage control. In order to achieve reliable operation, proper coordination between SGs and ESSs, as well as the characteristics of PPLs and associated control systems, have to be carefully studied.

Chapter 2 investigates the overall system configuration and control system in MVDC SMGs. The system architecture, shipboard functional blocks, and power converters are reviewed through which the function blocks are coupled into one integrated system. Three system architectures, and different types of power components, including generators, ESS, and propulsion motors, are compared from the aspects of critical features in each category. In terms of the control system in SMGs, the typical coordinated control methods, stability analysis, and protection systems are discussed. It is noteworthy that the control issues have to consider the effects of PPLs as they introduce special characters to the system. Thus, it is still a challenge in stability analysis and protection system design in the presence of PPLs.

Chapter 3 presents the solution to solve the first research question this thesis works on: a coordinated control strategy between the paralleled SGs and ESSs based on droop control. Two operation modes are considered according to ship working conditions to determine the operation principle, and the SoC of BESSs is considered in droop coefficient regulation to achieve SoC balance. Both the two operation modes and the mode shifting under the proposed coordinated control are verified by simulation results. The SoC balancing method is also illustrated to be effective.

The second research question this thesis focuses on is discussed in Chapter 4. Firstly, the characteristics of PPLs and the impacts of PPL parameters on the bus voltage are assessed by time-domain simulation. Afterwards, an improved method is developed for the PPS to mitigate this impact and supply the load effectively. The presented approach is based on the SMC, which has merits in dynamic response and

robustness to measurement noises. Comparisons with conventional PI control-based methods verify the effectiveness of the presented method.

5.2. MAIN CONTRIBUTIONS

Based on the above summaries, the main contributions of this thesis are drawn:

- **A comprehensive overview of MVDC SMGs.**
  This thesis reviews both the hardware and software issues in MVDC SMGs. The system architectures, various types of PGMs, ESSs, propulsion motors, and power converter topologies, including rectifiers, inverters, and DC/DC converters, are summarized and compared. Likewise, the software issues include control strategies, stability analysis, and protection schemes. Special considerations in developing the control strategies, analyzing the stability, and designing the protection schemes for MVDC SMGs are discussed.
- **A coordinated control strategy for SGs and BESSs.**
  Regarding the coordinated control, a droop control-based coordinated control strategy is presented for DC bus voltage regulation and power sharing between the SGs and BESSs in a MVDC SMG. Both hybrid-electric and all-electric operation modes are considered, and smooth mode shifting can be achieved. Besides, a SoC balancing method for achieving fast SoC balance between battery packs is developed.
- **An improved control method for PPS.**
  Regarding the PPS, the impacts of PPL profile on the bus voltage of MVDC SMGs are investigated, including the pulse duration, pulse interval time, and entire pulse time. Aiming at mitigating the adverse impacts of the PPL, the control principle of PPS and system design are presented. Furthermore, an improved control method based on SMC is developed to achieve fast voltage regulation and current tracking as well as robustness to measurement noises.

5.3. FUTURE RESEARCH PERSPECTIVES

Besides the outcomes in this Ph.D. project, there are still some issues on MVDC SMGs needing further development. Also, the overview of MVDC SMGs opens up several potential research directions. Future research perspectives are summarized as follows:

- Optimized sizing of SGs and ESSs is needed to have a cost-efficient operation. This Ph.D. project presents a coordination strategy for SGs and BESSs to achieve an efficient operation in different conditions, and the

SGs are controlled to output constant power. However, variable-speed SGs are allowed to fit the load conditions at the cost of the surplus SG capacities. Therefore, it is desired to optimize the proper capacity of SGs and ESSs and coordinate them for proper power sharing to achieve an overall reduced cost.

- Stability issues on PPLs need to be studied. In addition to providing solutions by adding energy storage devices to mitigate the negative impacts of PPLs like this Ph.D. project does, stability analysis on PPLs in a wide operation range is required to evaluate the control methods qualitatively.
- The protection system in DC SMGs needs to be studied to obtain high reliability. As discussed in Chapter 2, besides the general challenges in the DC system protection, the presence of PPLs introduce difficulties in fault detection with more possibility of triggering the breakers incorrectly.
- Intelligent shore-to-ship power connections should be investigated to achieve fast and efficient charging for electric ships. The charging power for ships is much higher than for electric vehicles, and the charging time is limited, making the shore-to-ship power supply a challenge. In addition to the charging strategies, the power conversion topologies with high power density are desired to make the connection more compact.

REFERENCES

[1] European Commissions, “2030 Climate Target Plan,” *EU Climate Action*, 2021. [Online]. Available: https://ec.europa.eu/clima/eu-action/european-green-deal/2030-climate-target-plan_en.

[2] European Commission, “Paris Agreement,” *EU Climate Action*, 2015. [Online]. Available: https://ec.europa.eu/clima/eu-action/international-action-climate-change/climate-negotiations/paris-agreement_en.

[3] M. Kammerer, “Fuel Cells for Marine Vessels: Why the Time to Transition Is Now,” 2021. [Online]. Available: https://blog.ballard.com/marine-fuel-cell.

[4] Arjen Kersing and Matt Stone, “Charting global shipping’s path to zero carbon,” 2022.

[5] Europan Maritime Safety Agency (EMSA)/European Environmental Agency (EEA), “European Maritime Transport Environmental Report 2021,” 2021.

[6] International Maritime Organization, “IMO Action to Reduce Greenhouse Gas Emissions from International Shipping,” 2019.

[7] European Environment Agency, “EU maritime transport: first environmental impact report acknowledges good progress towards sustainability and confirms that more effort is needed to prepare for rising demand,” 2021. [Online]. Available: https://www.eea.europa.eu/highlights/eu-maritime-transport-first-environmental.

[8] Helge Hermundsgård, “Norway challenges the cruise industry to operate emission free,” *DNV Maritime Impact*, 2019. [Online]. Available: https://www.dnv.com/expert-story/maritime-impact/Norway-challenges-the-cruise-industry-to-operate-emission-free.html.

[9] Statista, “Size of the European market for electric cargo ships from 2018 to 2020, with a forecast through 2030, by ship type,” *Europe Electric Ship Market Research Report*, 2020. [Online]. Available: https://www.statista.com/statistics/1278056/european-electric-cargo-ship-market-size-by-ship-type/.

[10] Fortune Business Insigts, “Electric Ships Market Size, Share and Covid-19 Impact Analysis,” 2020. [Online]. Available:

https://www.fortunebusinessinsights.com/electric-ships-market-104444.

[11] R. D. Geertsma, R. R. Negenborn, K. Visser, and J. J. Hopman, "Design and control of hybrid power and propulsion systems for smart ships: A review of developments," *Appl. Energy*, vol. 194, pp. 30–54, 2017.

[12] Stena Line, "Stena Line introduces battery power," 2019. [Online]. Available: https://www.stenalinefreight.com/news/stena-line-introduces-battery-power/.

[13] Marketsandmarkets, "Electric Ship Market by Type (Fully Electric, Hybrid), System, Mode of Operation (Manned, Remotely Operated, Autonomous), Ship Type (Commercial, Defense), Power, Range, Tonnage, End Use (Linefit and Retrofit), and Region - Global Forecast to 2030," 2020. [Online]. Available: https://www.marketsandmarkets.com/Market-Reports/electric-ships-market-167955093.html.

[14] Wärtsilä Marine, "Full electric vessels," 2020. [Online]. Available: https://www.wartsila.com/marine/build/electrical-and-power-systems/full-electric-vessels.

[15] F. Youd, "Crewless cargo: the world's first autonomous electric cargo ship," *Ship Technology*, 2022. [Online]. Available: https://www.ship-technology.com/analysis/crewless-cargo-the-worlds-first-autonomous-electric-cargo-ship/#:~:text=The world's first fully electric,its maiden voyage in Norway.

[16] ETHW, "Edison's Electric Light and Power System." [Online]. Available: https://ethw.org/Edison%27s_Electric_Light_and_Power_System.

[17] E. Skjong, E. Rødskar, and M. Molinas, "The Marine Vessel's Electrical Power System: From its Birth to Present Day," *Proc. IEEE*, vol. 103, no. 12, pp. 2410–2424, 2015.

[18] D. Bosich, A. Vicenzutti, and R. Pelaschiar, "Toward the future: The MVDC large ship research program," in *2015 AEIT International Annual Conference*, 2015.

[19] T. J. McCoy, "Integrated Power Systems - An Outline of Requirements and Functionalities for Ships," *Proc. IEEE*, vol. 103, no. 12, pp. 2276–2284, 2015.

[20] A. Rolan, P. Manteca, R. Oktar, and P. Siano, "Integration of Cold Ironing and Renewable Sources in the Barcelona Smart Port," *IEEE Trans. Ind. Appl.*, vol. 55, no. 6, pp. 7198–7206, 2019.

[21] ABB Review, “Shore-to-ship power,” *ABB Review*, 2010.

[22] B. Stevens, A. Dubey, and S. Santoso, “On Improving Reliability of Shipboard Power System,” *IEEE Trans. Power Syst.*, vol. 30, no. 4, pp. 1905–1912, 2015.

[23] C. R. Lashway, A. T. Elsayed, and O. A. Mohammed, “Hybrid energy storage management in ship power systems with multiple pulsed loads,” *Electr. Power Syst. Res.*, vol. 141, pp. 50–62, 2016.

[24] G. Sulligoi, A. Tessarolo, and V. Benucci, “Shipboard power generation: Design and development of a medium-voltage dc generation system,” *IEEE Ind. Appl. Mag.*, vol. 19, no. 4, pp. 47–55, 2013.

[25] J. Han, J. F. Charpentier, and T. Tang, “State of the art of fuel cells for ship applications,” in *IEEE International Symposium on Industrial Electronics*, 2012, pp. 1456–1461.

[26] T. Dragičević, X. Lu, J. C. Vasquez, and J. M. Guerrero, “DC Microgrids - Part II: A Review of Power Architectures, Applications, and Standardization Issues,” *IEEE Trans. Power Electron.*, vol. 31, no. 5, pp. 3528–3549, 2016.

[27] M. U. Mutarraf, Y. Terriche, and K. A. K. Niazi, “Energy storage systems for shipboard microgrids—A review,” *Energies*, vol. 11, no. 3492, pp. 1–32, 2018.

[28] R. Daiyan, I. MacGill, and R. Amal, “Opportunities and Challenges for Renewable Power-to-X,” *ACS Energy Lett.*, vol. 5, no. 12, pp. 3843–3847, 2020.

[29] SIEMENS Gamesa, “Industrial Decarbonization using Electric Thermal Energy Storage (ETES),” 2020. [Online]. Available: https://www.siemensgamesa.com/en-int/products-and-services/hybrid-and-storage/thermal-energy-storage-with-etes-add.

[30] V. A. Boicea, “Energy storage technologies: The past and the present,” *Proc. IEEE*, vol. 102, no. 11, pp. 1777–1794, 2014.

[31] American National Standards Institute, “IEEE Recommended Practice for 1 kV to 35 kV Medium-Voltage DC Power Systems on Ships,” 2010.

[32] J. Faber, D. Nelissen, and G. Hon, “Regulated Slow Steaming in Maritime Transport - An Assessment of Options, Costs and Benefits,” 2012.

[33] D. Perkins, T. Vu, and H. Vahedi, “Distributed power management implementation for zonal MVDC ship power systems,” in *Proceedings: IECON 2018 - 44th Annual Conference of the IEEE Industrial Electronics Society*, 2018, vol. 1, pp. 3401–3406.

[34] T. Goya, K. Uchida, and Y. Kinjyo, “Coordinated control of energy storage system and diesel generator in isolated power system,” in *IEEE 2nd International Power and Energy Conference*, 2008, pp. 925–930.

[35] X. Zhao-xia, Z. Tianli, and L. Huaimin, “Coordinated Control of a Hybrid-Electric-Ferry Shipboard Microgrid,” *IEEE Trans. Transp. Electrif.*, vol. 5, no. 3, pp. 828–839, 2019.

[36] H. M. Hasanien, “Design optimization of PID controller in automatic voltage regulator system using taguchi combined genetic algorithm method,” *IEEE Syst. J.*, vol. 7, no. 4, pp. 825–831, 2013.

[37] Z. Jin, L. Meng, and J. M. Guerrero, “Hierarchical control design for a shipboard power system with DC distribution and energy storage aboard future more-electric ships,” *IEEE Trans. Ind. Informatics*, vol. 14, no. 2, pp. 703–714, 2018.

[38] P. Xie, S. Tan, and N. Bazmohammadi, “A distributed real-time power management scheme for shipboard zonal multi-microgrid system,” *Appl. Energy*, vol. 317, 2022.

[39] Z. Zhou, M. B. Camara, and B. Dakyo, “Coordinated power control of variable-speed diesel generators and lithium-battery on a hybrid electric boat,” *IEEE Trans. Veh. Technol.*, vol. 66, no. 7, pp. 5775–5784, 2017.

[40] L. Xu and D. Chen, “Control and operation of a DC microgrid with variable generation and energy storage,” *IEEE Trans. Power Deliv.*, vol. 26, no. 4, pp. 2513–2522, 2011.

[41] Z.-X. Xiao, H.-M. Li, and H.-W. Fang, “Operation Control for Improving Energy Efficiency of Shipboard Microgrid Including Bow Thrusters and Hybrid Energy Storages,” *IEEE Trans. Transp. Electrif.*, vol. 6, no. 2, pp. 856–868, 2020.

[42] M. Aizza, D. Bosich, and S. Castellan, “Coordinated speed and voltage regulation of a DC power generation system based on a woundfield split-phase generator supplying multiple rectifiers,” in *6th IET International Conference on Power Electronics, Machines and Drives (PEMD)*, 2012.

[43] S. Kulkarni and S. Santoso, “Impact of pulse loads on electric ship power system: With and without flywheel energy storage systems,” *IEEE Electr. Sh. Technol. Symp. ESTS 2009*, pp. 568–573, 2009.

[44] B. Vural and C. S. Edrington, “Ultra-Capacitor Based Pulse Power Management in Electrical Ships,” in *2012 IEEE Transportation Electrification Conference and Expo (ITEC)*, 2012.

[45] J. J. A. van der Burgt, P. van Gelder, and E. van Dijk, “Pulsed power requirements for future naval ships,” in *Digest of Technical Papers. 12th IEEE International Pulsed Power Conference*, 1999.

[46] M. M. Mardani, M. H. Khooban, and A. Masoudian, “Model Predictive Control of DC-DC Converters to Mitigate the Effects of Pulsed Power Loads in Naval DC Microgrids,” *IEEE Trans. Ind. Electron.*, vol. 66, no. 7, pp. 5676–5685, 2019.

[47] Z. Dong, X. Cong, and Z. Xiao, “A Study of Hybrid Energy Storage System to Suppress Power Fluctuations of Pulse Load in Shipboard Power System,” in *2020 International Conference on Smart Grids and Energy Systems (SGES)*, 2020, pp. 437–441.

[48] A. Birudula, R. Selvaraj, and K. Desingu, “A Coordinated Control Strategy for Diesel Electric Tugboat System for Improved Fuel Economy,” *IEEE Trans. Ind. Appl.*, vol. 56, no. 5, pp. 5439–5451, 2020.

[49] K. Mills, J. Xiong, X. Liu, and P. Venkatesh, “Informing the power system performance envelope for pulse load operation,” in *14th International Naval Engineering Conference & Exhibition*, 2018, pp. 1–14.

[50] K. Kim, K. Park, G. Roh, and K. Chun, “DC-grid system for ships: a study of benefits and technical considerations,” *J. Int. Marit. Safety, Environ. Aff. Shipp.*, vol. 2, no. 1, pp. 1–12, 2018.

[51] J. V. Amy, “Condiserations in the Design of Naval Electric Power Systems,” in *IEEE Power Engineering Society Summer Meeting*, 2002.

[52] A. K. Ådnanes, “Maritime electrical installations and diesel electric propulsion,” ABB, Oslo, 2003.

[53] G. Sulligoi, A. Tessarolo, and V. Benucci, “Modeling, simulation, and experimental validation of a generation system for medium-voltage DC integrated power systems,” *IEEE Trans. Ind. Appl.*, vol. 46, no. 4, pp. 1304–1310, 2010.

[54] L. Luckose, H. L. Hess, and B. K. Johnson, “Power conditioning system for fuel cells for integration to ships,” in *2009 IEEE Vehicle Power and Propulsion Conference*, 2009.

[55] M. Godjevac, K. Visser, and E. J. Boonen, “Electrical energy storage for dynamic positiong operations: Investigation of three application case,” in *2017 IEEE Electric Ship Technologies Symposium (ESTS)*, 2017.

[56] S. M. Mousavi G, F. Faraji, A. Majazi, and K. Al-Haddad, “A comprehensive review of Flywheel Energy Storage System technology,” *Renew. Sustain. Energy Rev.*, vol. 67, pp. 477–490, 2017.

[57] H. Louie and K. Strunz, “Superconducting Magnetic Energy Storage (SMES) for energy cache control in modular distributed hydrogen-electric energy systems,” *IEEE Trans. Appl. Supercond.*, vol. 17, no. 2, pp. 2361–2364, 2007.

[58] S. J. Park, J. H. Song, and H. Y. Choi, “A study on design of inverter for multi-phase brushless DC ship propulsion motor,” in *2010 IEEE Vehicle Power and Propulsion Conference*, 2010.

[59] A. Nanoty and A. R. Chudasama, “Control of Designed Developed Six Phase Induction Motor,” *Int. J. Electromagn. Appl.*, vol. 2, no. 5, pp. 77–84, 2012.

[60] J. L. Kirtley, A. Banerjee, and S. Englebretson, “Motors for Ship Propulsion,” *Proc. IEEE*, vol. 103, no. 12, pp. 2320–2332, 2015.

[61] J. S. Thongam, M. Tarbouchi, and A. F. Okou, “All-electric ships - A review of the present state of the art,” in *2013 8th International Conference and Exhibition on Ecological Vehicles and Renewable Energies (EVER)*, 2013.

[62] U. Javaid, “MVDC Supply Technologies for Marine Electrical Distribution Systems,” *CPSS Trans. Power Electron. Appl.*, vol. 3, no. 1, pp. 65–76, 2018.

[63] D. Dong, R. Lai, and Y. Pan, “Active fault-current foldback control in thyrister rectifier for DC shipboard electrical system,” in *2015 IEEE Electric Ship Technologies Symposium (ESTS)*, 2015.

[64] D. Ronanki, S. Member, S. S. Williamson, and S. Member, “Modular Multilevel Converters for Transportation Electrification : Challenges and Opportunities,” *IEEE Trans. Transp. Electrif.*, vol. 4, no. 2, pp. 399–407, 2018.

[65] Y. Chen, Z. Li, S. Zhao, X. Wei, and Y. Kang, “Design and Implementation of a Modular Multilevel Converter with Hierarchical Redundancy Ability for

Electric Ship MVDC System," *IEEE J. Emerg. Sel. Top. Power Electron.*, vol. 5, no. 1, pp. 189–202, 2017.

[66] F. Deng and Z. Chen, "A control method for voltage balancing in modular multilevel converters," *IEEE Trans. Power Electron.*, vol. 29, no. 1, pp. 66–76, 2014.

[67] ABB Ltd., "A Guide to standard medium voltage variable speed Drive," 2017. [Online]. Available: https://library.e.abb.com/public/4fb66e46af347939c1256ed800338956/Fact Packs Part2.pdf.

[68] K. Thantirige, A. K. Rathore, and S. K. Panda, "Medium voltage multilevel converters for ship electric propulsion drives," in *Electrical Systems for Aircraft, Railway and Ship Propulsion (ESARS)*, 2015.

[69] Q. Wei, L. Xing, and D. Xu, "Modulation Schemes for Medium-Voltage PWM Current Source Converter-Based Drives : An Overview," *IEEE J. Emerg. Sel. Top. Power Electron.*, vol. 7, no. 2, pp. 1152–1161, 2019.

[70] S. Kouro, M. Malinowski, and K. Gopakumar, "Recent advances and industrial applications of multilevel converters," *IEEE Trans. Ind. Electron.*, vol. 57, no. 8, pp. 2553–2580, 2010.

[71] W. You, Z. Zedong, and L. Yongdong, "DAB-based PET in MVDC traction and shipboard applications with distribution and redundant control," *J. Eng.*, vol. 2019, no. 16, pp. 3209–3213, 2019.

[72] D. Liu, F. Deng, and Z. Chen, "Five-Level Active-Neutral-Point-Clamped DC/DC Converter for Medium-Voltage DC Grids," *IEEE Trans. Power Electron.*, vol. 32, no. 5, pp. 3402–3412, 2017.

[73] G. Yang, F. Xiao, and X. Fan, "Three-Phase Three-Level Phase-Shifted PWM DC-DC Converter for Electric Ship MVDC Application," *IEEE J. Emerg. Sel. Top. Power Electron.*, vol. 5, no. 1, pp. 162–170, 2017.

[74] D. Fisher, R. C. Linger, and H. F. Lipson, "Survivable Network Systems: An Emerging Discipline," 1997.

[75] Z. Jin, L. Meng, J. C. Vasquez, and J. M. Guerrero, "Frequency-division power sharing and hierarchical control design for DC shipboard microgrids with hybrid energy storage systems," in *Conference Proceedings - IEEE Applied Power Electronics Conference and Exposition (APEC)*, 2017, pp. 3661–3668.

[76] F. Balsamo, P. De Falco, F. Mottola, and M. Pagano, "Power Flow Approach for Modeling Shipboard Power System in Presence of Energy Storage and Energy Management Systems," *IEEE Trans. Energy Convers.*, vol. 35, no. 4, pp. 1944–1953, 2020.

[77] T. Dragicevic, X. Lu, J. C. Vasquez, and J. M. Guerrero, "DC Microgrids - Part I: A Review of Control Strategies and Stabilization Techniques," *IEEE Trans. Power Electron.*, vol. 31, no. 7, pp. 4876–4891, 2016.

[78] A. Accetta and M. Pucci, "A first approach for the energy management system in dc micro-grids with integrated RES of smart ships," in *2017 IEEE Energy Conversion Congress and Exposition (ECCE)*, 2017.

[79] M. Banaei, M. Rafiei, J. Boudjadar, and M. H. Khooban, "A Comparative Analysis of Optimal Operation Scenarios in Hybrid Emission-Free Ferry Ships," *IEEE Trans. Transp. Electrif.*, vol. 6, no. 1, pp. 318–333, 2020.

[80] M. R. Hossain and H. L. Ginn, "Real-Time Distributed Coordination of Power Electronic Converters in a DC Shipboard Distribution System," *IEEE Trans. Energy Convers.*, vol. 32, no. 2, pp. 770–778, 2017.

[81] L. Meng *et al.*, "Review on Control of DC Microgrids," *IEEE J. Emerg. Sel. Top. Power Electron.*, pp. 1–1, 2017.

[82] G. Sulligoi, D. Bosich, and G. Giadrossi, "Multiconverter medium voltage DC power systems on ships: Constant-power loads instability solution using linearization via state feedback control," *IEEE Trans. Smart Grid*, vol. 5, no. 5, pp. 2543–2552, 2014.

[83] G. Sulligoi, D. Bosich, and L. Zhu, "Linearizing control of shipboard multi-machine MVDC power systems feeding Constant Power Loads," in *2012 IEEE Energy Conversion Congress and Exposition (ECCE)*, 2012.

[84] G. Sulligoi, D. Bosich, V. Arcidiacono, and G. Giadrossi, "Considerations on the design of voltage control for multi-machine MVDC power systems on large ships," *2013 IEEE Electr. Sh. Technol. Symp. ESTS 2013*, pp. 314–319, 2013.

[85] W. W. Weaver, R. D. Robinett, and D. G. Wilson, "Metastability of Pulse Power Loads Using the Hamiltonian Surface Shaping Method," *IEEE Trans. Energy Convers.*, vol. 32, no. 2, pp. 820–828, 2017.

[86] M. Kabalan, P. Singh, and D. Niebur, "Large Signal Lyapunov-Based Stability Studies in Microgrids: A Review," *IEEE Trans. Smart Grid*, vol. 8,

no. 5, pp. 2287–2295, 2017.

[87] G. Wang, R. Xiao, and C. Xu, “Stability analysis of integrated power system with pulse load,” *Int. J. Electr. Power Energy Syst.*, vol. 115, p. 105462, 2020.

[88] A. P. N. Tahim, D. J. Pagano, and E. Lenz, “Modeling and Stability Analysis of Islanded DC Microgrids under Droop Control,” *IEEE Trans. Power Electron.*, vol. 30, no. 8, pp. 4597–4607, 2015.

[89] Y. Tang and A. Khaligh, “On the feasibility of hybrid battery/ultracapacitor energy storage systems for next generation shipboard power systems,” in *2010 IEEE Vehicle Power and Propulsion Conference (VPPC)*, 2010.

[90] L. Tan, Q. Yang, and W. Im, “Adaptive critic design based cooperative control for pulsed power loads accommodation in shipboard power system,” *IET Gener. Transm. Distrib.*, vol. 10, no. 11, pp. 2739–2747, 2016.

[91] P. Lin and C. Zhang, “On Autonomous Large-Signal Stabilization for Islanded Multibus DC Microgrids: A Uniform Nonsmooth Control Scheme,” *IEEE Trans. Ind. Electron.*, vol. 67, no. 6, pp. 4600–4612, 2020.

[92] R. M. Cuzner and G. Venkataramanan, “The status of DC micro-grid protection,” in *IEEE Industry Applications Society Annual Meeting*, 2008.

[93] D. Bosich and G. Sulligoi, “Voltage control on a refitted luxury yacht using hybrid electric propulsion and LVDC distribution,” in *8th International Conference and Exhibition on Ecological Vehicles and Renewable Energies (EVER)*, 2013.

[94] Q. Deng, X. Liu, and R. Soman, “Primary and backup protection for fault current limited MVDC shipboard power systems,” in *IEEE Electric Ship Technologies Symposium (ESTS)*, 2015.

[95] P. Cairoli, L. Qi, and C. Tschida, “High Current Solid State Circuit Breaker for DC Shipboard Power Systems,” in *2019 IEEE Electric Ship Technologies Symposium (ESTS)*, 2019, pp. 468–476.

[96] K. Satpathi, A. Ukil, and J. Pou, “Short-Circuit Fault Management in DC Electric Ship Propulsion System: Protection Requirements, Review of Existing Technologies and Future Research Trends,” *IEEE Trans. Transp. Electrif.*, vol. 4, no. 1, pp. 272–291, 2017.

[97] R. Rajaram, K. S. Kumar, and N. Rajasekar, “Power system reconfiguration in a radial distribution network for reducing losses and to improve voltage

profile using modified plant growth simulation algorithm with Distributed Generation (DG),” *Energy Reports*, vol. 1, pp. 116–122, 2015.

[98] M. A. N. Guimarães, J. F. C. Lorenzeti, and C. A. Castro, “Reconfiguration of distribution systems for voltage stability margin enhancement using tabu search,” in *International Conference on Power System Technology, PowerCon 2004*, 2004, vol. 2, pp. 1556–1561.

[99] X. Lu, K. Sun, and J. M. Guerrero, “Double-quadrant state-of-charge-based droop control method for distributed energy storage systems in autonomous DC Microgrids,” *IEEE Trans. Smart Grid*, vol. 6, no. 1, pp. 147–157, 2015.

[100] H. Kifune, M. K. Zadhe, and H. Sasaki, “Efficiency estimation of synchronous generators for marine applications and verification with shop trial data and real ship operation data,” *IEEE Access*, vol. 8, pp. 195541–195550, 2020.

[101] E. L. Neau, “High average power, high current pulsed accelerator technology,” *Proc. IEEE Part. Accel. Conf.*, vol. 2, pp. 1188–1192, 1995.

[102] L. N. Domaschk, A. Ouroua, R. E. Hebner, O. E. Bowlin, and W. B. Colson, “Coordination of large pulsed loads on future electric ships,” *IEEE Trans. Magn.*, vol. 43, no. 1, pp. 450–455, 2007.

[103] X. Huang, X. Ruan, F. Du, F. Liu, and L. Zhang, “A Pulsed Power Supply Adopting Active Capacitor Converter for Low-Voltage and Low-Frequency Pulsed Loads,” *IEEE Trans. Power Electron.*, vol. 33, no. 11, pp. 9219–9230, 2018.

[104] X. Gao, H. Wu, S. Member, S. Gao, Z. Zhang, and Y. Xing, “A Two-Stage Pulsed Power Supply for Low-DC-Voltage and Low-Frequency Pulsed-Current Loads,” *IEEE Trans. Power Electron.*, vol. 36, no. 2, pp. 2298–2309, 2021.

[105] C. Lascu, “Sliding-Mode Direct-Voltage Control of Voltage-Source Converters with LC Filters for Pulsed Power Loads,” *IEEE Trans. Ind. Electron.*, vol. 68, no. 12, pp. 11642–11650, 2021.

[106] M. Steurer, M. Andrus, and J. Langsten, “Investigating the impact of pulsed power charging demands on shipboard power quality,” in *IEEE Electric Ship Technologies Symposium (ESTS)*, 2007.

ISSN (online): 2446-1636
ISBN (online): 978-87-7573-840-3

AALBORG UNIVERSITY PRESS